TABLE 2 Percent homology between JFH-2 and other genotype 2a strains

Region	JFH-2 nucleotide profile				JFH-2 amino acid profie			
	Lenght (nt)[a]	% Identity vs strain:			Length (aa)[b]	% Amino acid identity vs strain:		
		JFH-1	J6CF	JCH-1		JFH-1	J6CF	JCH-1
Entire genome	9683	87.60	88.98	88.88	3033	90.64	91.79	91.79
UTR[c]	576	96.35	98.61	96.88	NA[d]			
Structural	2439	86.14	87.90	86.51	813	89.30	89.54	88.56
Nonstructural	6663	87.44	88.59	89.12	2220	91.13	92.61	92.97
5′ UTR	340	98.82	99.71	99.71	NA			
Core	573	91.80	93.02	91.97	191	92.15	95.29	92.15
E1	576	87.50	88.89	89.06	192	90.10	92.19	89.58
E2-p7	1290	83.02	85.19	82.95	430	87.67	85.81	86.51
NS2	651	84.18	85.87	89.09	217	87.56	88.02	91.24
NS3	1893	87.64	88.54	89.33	631	92.87	94.61	94.45
NS4A	162	88.27	88.27	88.27	54	96.30	92.59	94.44
NS4B	783	89.91	90.04	89.14	261	96.93	97.32	96.55
NS5A	1398	83.48	85.98	85.48	466	82.83	86.70	86.48
NS5B	1776	90.37	91.10	91.84	591	94.08	94.75	95.43
3′ UTR	236	92.80	97.03	92.80	NA			

[a] nt, nucleotides.
[b] aa, amino acids.
[c] UTR, 5′ UTR plus 3′ UTR.
[d] NA, not applicable.

positions of different amino acid sequences of each strain (Fig. 3A). The E2 and NS5A regions are more variable than other regions (Fig. 3A and Table 2); however, it is difficult to find particular mutation positions or regions specific for the JFH-2 strain.

Subgenomic replicon analysis of the JFH-2 clone. Interestingly, some parts of the viral cDNA sequences in the JFH-2 viral genome were a mixture of different sequences, especially in the NS3 region. By the cloning analysis, we found two major se-

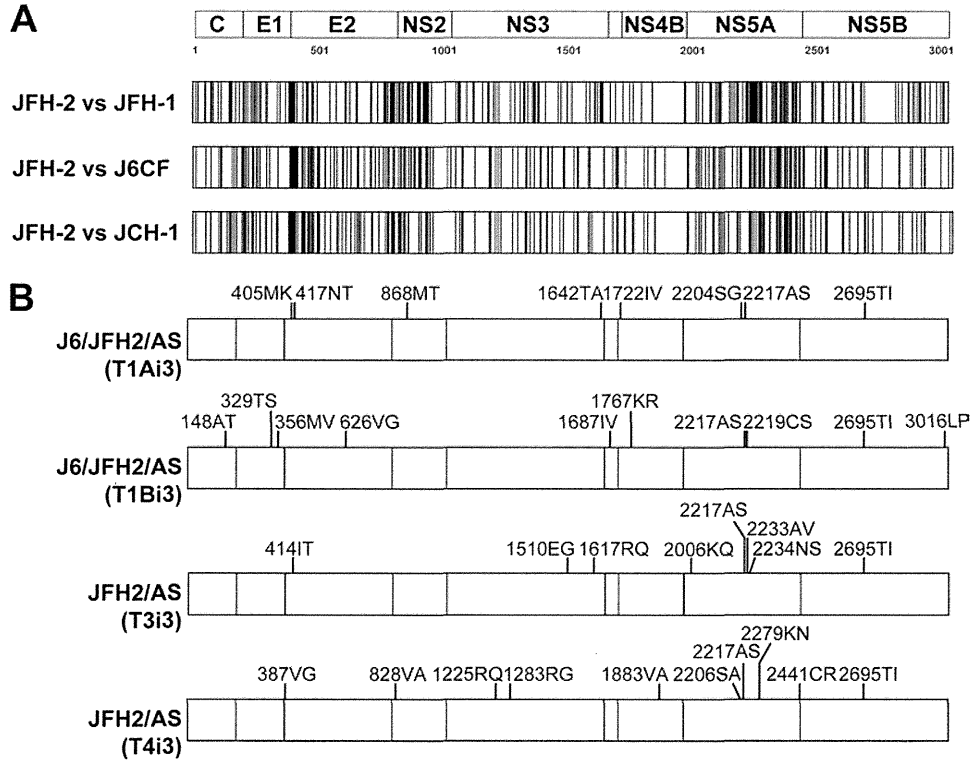

FIG 3 Maps of amino acid sequences among genotype 2a HCV strains and mutations found in the cell culture-adapted viruses. (A) Amino acid sequences of the entire open reading frame (3,033 amino acids) of JFH-1, JFH-2, J6CF (accession numbers AB047639, AB690461, and AF177036, respectively), and JCH-1 strains were compared. The positions of different sequences are indicated by vertical lines. (B) Virus genome sequences were determined in the T1Ai3 and T1Bi3 culture media of the J6/JFH2/AS virus-inoculated cells or T3i3 and T4i3 culture media of the JFH2/AS virus-inoculated cells, as described in the text. Amino acid mutations are indicated with their positions and residues.

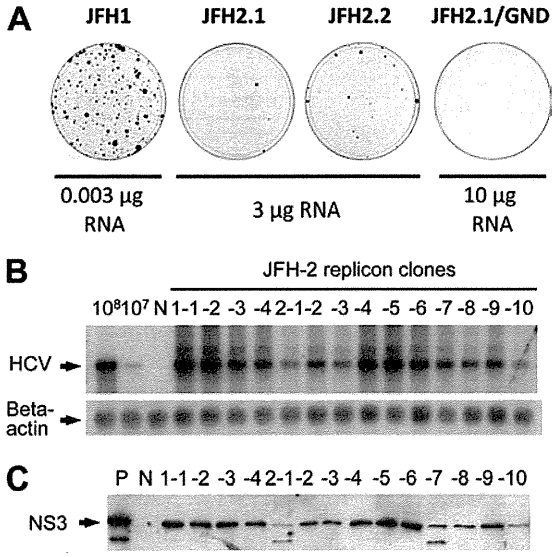

FIG 4 G418-resistant colony formation of JFH-1 and JFH-2 replicons and analysis of JFH-2 replicon cells. (A) Subgenomic RNAs were synthesized *in vitro* by using pSGR-JFH1, pSGR-JFH2.1, pSGR-JFH2.2, and pSGR-JFH2.1/GND as templates. Transcribed subgenomic RNAs were electroporated into HuH-7 cells, and cells were cultured with G418 for 3 weeks before being stained with crystal violet. JFH-1 subgenomic RNA (0.003 μg), 3 μg of JFH-2.1 and JFH-2.2 subgenomic RNA, and 10 μg of JFH-2.1/GND subgenomic RNA were transfected into HuH-7 cells. Experiments were performed in triplicate, and representative staining examples are shown. (B) Northern blot analysis. Total cellular RNA isolated from each of four SGR-JFH2.1 clones (1-1 to 1-4) and 10 SGR-JFH2.2 clones (2-1 to 2-10) was analyzed by using a random-primed DNA probe to detect replicon RNA. Isolated total cellular RNA (4 μg) was separated by denatured agarose gel electrophoresis. After electrophoresis, HCV- and beta-actin-specific RNAs were detected by Northern blot analysis with random-primed DNA probes specific to HCV and beta-actin sequences. Arrows indicate replicon RNA or beta-actin mRNA. (C) Western blot analysis. Cell lysates were prepared from four SGR-JFH2.1 clones (1-1 to 1-4) and 10 SGR-JFH2.2 clones (2-1 to 2-10). The NS3 proteins were detected with rabbit anti-HCV NS3 antibody. Positive-control (P) and negative-control (N) cell lysates were obtained from JFH-1 replicon cells and naive HuH-7 cells.

quences in the JFH-2 viral genome. One sequence contained alanine and isoleucine (AI) at amino acid positions 1204 and 1205, and the other contained methionine and leucine (ML) at the same positions. We referred to these viral genomes containing AI or ML as JFH-2.1 or JFH-2.2, respectively. From the cloning analysis of PCR products, JFH-2.1 populated 19 of 32 clones (59%), and JFH-2.2 populated 13 of 32 clones (41%). To analyze the replication efficiency of the JFH-2 clone, we thus constructed two subgenomic replicon constructs, pSGR-JFH2.1 and pSGR-JFH2.2, as pSGR-JFH1 (11). Synthesized replicon RNAs of JFH-2.1 and JFH-2.2 were independently transfected by electroporation into HuH-7 cells. The transfected cells were then grown for 3 weeks in selection culture that contained 1 mg/ml of G418. Several colonies survived the selection culture, as illustrated by crystal violet staining (Fig. 4A). The JFH2.1/GND replication-incompetent control RNA-transfected cells did not form any colonies, even when 10 μg of RNA was transfected. The colony formation efficiencies of the JFH-2.1 and JFH-2.2 replicons were 0.94 ± 0.54 and 6.43 ± 3.39 CFU/μg RNA, respectively, which were substantially lower than the colony formation efficiency of the JFH-1 subgenomic replicon ($5.32 \times 10^4 \pm 5.02 \times 10^4$ CFU/μg RNA) (11). Four colonies of the JFH-2.1 replicon and 10 colonies of the JFH-2.2 replicon were cloned and expanded for further analysis. Replicon RNA was isolated from each replicon cell clone, and the HCV RNA titer and sequence of the replicon genome were determined (Table 3). The average HCV RNA titer in replicon cell clones was determined by real-time RT-PCR detection as (8.70 ± 4.94) $\times 10^7$ copies/μg of RNA. The size and amount of the replicon RNA in the replicon cells were confirmed by Northern blot analysis (Fig. 4B). We also detected NS3 protein in each clone of replicon cells by Western blot analysis (Fig. 4C). NS3 proteins were mainly found at approximately 70-kDa by polyclonal anti-NS3 antibody; however, an additional signal was also detected at a smaller molecular size in some replicon cells, including the positive-control JFH-1 replicon cells.

Next, we determined the sequences of replicating RNA in each replicon cell clone. Most of the clones, except replicon clone 2.2-8, had at least one nonsynonymous mutation (Table 3). We found nonsynonymous mutations in the NS3, NS5A, and NS5B regions, and three mutations were common among the different replicon genomes. Among the mutations found in the NS3 region, both 1547FL and 1614CW were found in two different replicon cells, and the 1651TN mutation was found in five replicon cells. The 2280QR mutation in NS5A was found in three replicon cells. 2217AS and 2222HQ, which are located in the interferon sensitivity-determining region (ISDR), were each found in a single replicon cell (8). To determine the adaptive effect of these mutations (Fig. 5A), we inserted these mutations (listed in Table 3), except for 1204MK, into pSGR-JFH2.1 and tested the colony formation efficiency of the mutant replicons. The 1204MK mutation was not tested since methionine at amino acid position 1204 was specific for the JFH2.2 sequence. As shown in Fig. 5B, 1547FL, 1614CW, 1651TN, 2222HQ, and 2280QR had weak to moderate adaptive effects for colony formation. Interestingly, the 2217AS mutation in the ISDR strongly enhanced the colony formation to approximately 3×10^4 times that of the parental JFH2.1 replicon (Fig. 5B). We further tested these adaptive mutations in the luciferase reporter replicon format, as described previously (12). SGR-JFH2.1 with the 2217AS construct exhibited significant replication compared to JFH2.1/GND, which is the replication-incompetent negative control. However, other constructs showed no evidence of replication in the transient replication assay (Fig. 5C).

Full-length HCV replication. The 2217AS mutation substantially enhanced RNA replication of the JFH-2.1 subgenomic replicon compared with other mutations. We examined whether a full-length JFH-2 HCV clone with the 2217AS mutation could produce infectious virus. In our previous study, we constructed the J6/JFH1 chimeric construct by replacement of the 5′ untranslated region to the p7 region (EcoRI-BclI) of J6 (1), and we found that J6/JFH1 produces a larger amount of infectious virus in the culture medium (3). We thus used the structural region of the J6CF clone and the NS2 region of the JFH-1 clone from a J6/JFH-1 chimeric virus construct and fused it to the NS3 to 3′X regions of JFH-2.1 with the 2217AS mutation (plasmid pJ6/JFH2/AS) since it was not clear if the structural and NS2 regions of the JFH-2 strain were functionally intact (Fig. 6A). Full-length viral RNA was synthesized from linearized pJ6/JFH2/AS and electroporated into Huh-7.5.1 cells. After two independent transfections, the transfected cells were divided into sub-cell lines to form a total of four sub-cell lines (T1A, T1B, T2A, and T2B). All four sub-cell lines were serially passaged, and HCV core protein, RNA, and infectivity levels in the culture supernatant were monitored (Fig.

TABLE 3 Mutations and RNA titer of the JFH-2 replicon cell clones

Replicon clone	Nucleotide		Amino acid			Replicon titer (no. of copies/μg of RNA)
	Mutation	Position	Mutation	Position	Region	
2.1-1	A→G	2012	E→G	1109	NS3	1.30E+8
	C→A	3638	T→N	1651	NS3	
2.1-2	T→C	3325	F→L	1547	NS3	1.52E+8
	C→A	3638	T→N	1651	NS3	
2.1-3	A→G	5525	Q→R	2280	NS5A	1.09E+8
	A→G	7155	None		NS5B	
2.1-4	C→A	3638	T→N	1651	NS3	1.41E+8
	A→G	7795	None		3′ UTR	
2.2-1	C→G	3528	C→W	1614	NS3	2.33E+7
2.2-2	G→T	5335	A→S	2217	NS5A (ISDR)	3.57E+7
2.2-3	C→G	919	None		*neo*	3.35E+7
	C→A	5352	H→Q	2222	NS5A (ISDR)	
2.2-4	C→A	1223	None		EMCV-IRES[a]	1.05E+8
	C→A	2115	None		NS3	
	G→T	6243	K→N	2519	NS5B	
2.2-5	C→A	3327	F→L	1547	NS3	1.67E+8
2.2-6	T→C	625	None		*neo*	1.09E+8
	C→A	3638	T→N	1651	NS3	
	A→G	5525	Q→R	2280	NS5A	
	T→A	5754	None		NS5A	
	G→A	5803	G→S	2373	NS5A	
2.2-7	C→G	3528	C→W	1614	NS3	6.25E+7
2.2-8	None		None			5.31E+7
2.2-9	C→G	3638	T→N	1651	NS3	6.71E+7
	G→A	5269	A→T	2195	NS5A	
	A→G	5525	Q→R	2280	NS5A	
2.2-10	T→A	2297	M→K	1204	NS3	2.95E+7
	A→G	7815	None		3′ UTR	

[a] EMCV-IRES, encephalomyocarditis virus internal ribosome entry site.

6B and C and Table 4). At the first cell passage, the HCV core protein levels were approximately 300 fmol/liter, and the infectivities were very low. Secreted HCV core protein levels decreased in all of the passaged cells until 25 days after the transfection. However, HCV core protein secretion of passaged T1A cells began to increase from 30 days after transfection. Subsequently, increased core protein secretion was also observed in other passaged cells although at different time points (Fig. 6B and Table 4). The maximum core protein levels in the medium were up to 9,241 fmol/liter in T1B cells at day 75 posttransfection. Infectivity detected in the culture medium was also first increased in T1A, and similar increases were observed with other passaged cells at later time points. Furthermore, specific infectivity (infectivity/HCV RNA or infectivity/HCV core protein) was also higher than in the initial culture medium (Table 4). The passaged cells were immunostained with anti-core monoclonal antibody (Fig. 6D). At 4 weeks after transfection, only a few cells were positive in all four sub-cell lines. However, the number of positive cells increased from 8, 12, 18, or 14 weeks after transfection in T1A, T1B, T2A, or T2B cells, respectively. These results indicate that phenotypic change occurred in the replicating virus after the serial passages of the transfected cells. Before this phenotypic change, the replicating viruses were not able to secrete significant amounts of infectious virus particles due to an unknown defect in infectious virus particle formation or secretion. After the phenotypic change, the robust core protein secretion might have been caused by changes in the efficiency of infectious virus production or secretion. To compare the virus characteristics before and after the phenotypic change, we analyzed T1A culture medium from 5 days, 8 weeks, and 11 weeks posttransfection by density gradient assay (Fig. 6E). The day 5 medium showed a broad density profile both of core protein and HCV RNA, and infectivity was not detected. Interestingly, the peaks of HCV core protein and RNA at around 1.15 mg/ml density became higher at 8 weeks and had a further increase at 11 weeks. Broader minor peaks at the lighter density remained small at week 11. The infectivity peak also became higher at 8 and 11

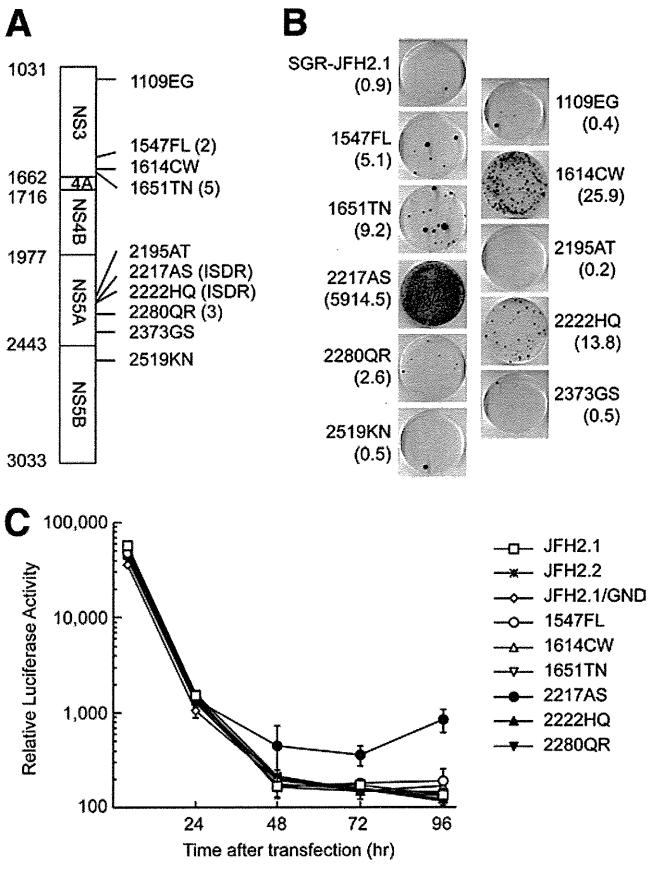

FIG 5 Analysis of the effect on colony formation and transient replication efficiency of mutations detected in replicon cell clones. (A) The box indicates the open reading frame of JFH-2 replicon and amino acid sequences at positions 1031 and 3033 (numbering by full-length JFH-2). The numbers on the left side of the box show the starting position of each protein, with the exception of 3033, which is the end position of NS5B. The numbers with the lines on the right side indicate the mutations introduced in the replicon constructs. 1547FL, 1651TN, and 2280QR mutations were found in 2, 5, and 3 replicon clones, respectively (Table 3). 2217AS and 2222HQ mutations were found in the ISDR (Table 3). (B) Each amino acid mutation found in the replicon genome was introduced into the pSGR-JFH2.1 replicon construct, and colony formation of the JFH2.1 replicon with the wild-type sequence (SGR-JFH2.1) and other mutations was tested. Briefly, transcribed RNA (5 μg) was transfected into HuH-7 cells, and cells were cultured for 3 weeks before being stained with crystal violet. The numbers in the parentheses show the colony formation efficiency (CFU/μg of RNA) of the replicon constructs. (C) Transient replication of JFH-2 subgenomic replicon. HuH-7 cells were transfected with the transcribed RNA from pSGR-JFH2.1/Luc, pSGR-JFH2.2/Luc, pSGR-JFH2.1/Luc/GND (replication-incompetent control), and pSGR-JFH2.1/Luc constructs with adaptive mutations (1547FL, 1614CW, 1651TN, 2217AS, 2222HQ, and 2280QR). Transfected cells were harvested at the indicated time points and at 4 h posttransfection. Relative luciferase activity (arbitrary units) was measured in the cell lysate. Assays were performed in triplicate, and data are presented as means ± standard deviations. The background signal of the luciferase measurement was 129.4 ± 27.4 units.

weeks after transfection. Interestingly, this density profile at 11 weeks posttransfection was quite similar to that of JFH-1 or the J6/JFH1 chimera, as previously described (21, 38). Furthermore, virus-like particles were visualized in the concentrated culture medium by electron microscopic analysis, whereas only unstructured aggregates were found with the mock-transfected control (Fig. 7, left panel; also data not shown). An aliquot of the culture medium was used for immunoelectron microscopy with an E2-specific antibody (AP33), and gold-labeled spherical structures were detected (Fig. 7, middle panel). The overall diameter of the structures (50 to 65 nm) is compatible with the predicted size of HCV.

Characterization of cell culture-adapted J6/JFH2/AS virus. During the serial passages of the transfected cells, the J6/JFH2/AS virus adapted to produce more infectious viruses in the cell culture. We next compared the adapted J6/JFH2/AS virus (T1B cells at day 75 posttransfection) with the J6/JFH1 virus. Huh-7.5.1 cells were inoculated with the viruses at a multiplicity of infection (MOI) of 0.03. The core protein production levels in both the infected cells and the culture medium were increased with similar kinetics after the virus infection, although at lower levels for J6/JFH2/AS virus than J6/JFH1 virus (Fig. 8A). We also tested the neutralization of the infection of these viruses by using mouse anti-CD81 monoclonal antibody and anti-HCV human IgG purified from HCV carrier serum (Fig. 8B). Both antibodies clearly inhibited the infectivity of inoculated virus to Huh-7.5.1 cells. Thus, the J6/JFH2/AS and J6/JFH1 viruses appeared to share similar infection pathways.

Adaptive mutations in the cell culture-adapted J6/JFH2.2/AS virus. We determined the full-length sequence of the HCV genome in the culture medium of T1A and T1B sub-cell lines at 75 days posttransfection by directly sequencing the amplified virus cDNA. We found the following nonsynonymous mutations, in addition to 2217AS, in the viral genomes: 1342ST in NS3 and 2219CR in NS5A of T1A and 148AT in the core protein, 2219CS in NS5A, and 2695TI and 3016LP in NS5B of T1B. These mutations were introduced into the J6/JFH2.2/AS cDNA, and synthetic RNA was transfected into Huh-7.5.1 cells. However, robust virus production was not observed at an early time point after transfection (data not shown). Because the important adaptive mutations might still not be detected in the virus population, we decided to concentrate on the dominant virus population and fix the important mutations in T1A and T1B virus by serial virus passages. We thus repeatedly inoculated naive Huh-7.5.1 cells three times with J6/JFH2/AS virus at a low MOI and harvested the virus when the virus titer plateaued. We sequenced the full-length genome of virus in the culture medium after the third inoculation (T1Ai3 or T1Bi3) and found the following nonsynonymous mutations: 405MK and 417NT in E2, 868MT in NS2, 1642TA in NS3, 1722IV in NS4B, 2204SG in NS5A, and 2695TI in NS5B of T1Ai3; and 148AT in the core protein, 329TS and 356MV in E1, 626VG in E2, 1678IV in NS4A, 1767KR in NS4B, 2219CS in NS5A, and 2695TI and 3016LP in NS5B of T1Bi3 (Fig. 3B). We then introduced these mutations into pJ6/JFH2/AS to construct pJ6/JFH2/AS/mtT1A and pJ6/JFH2/AS/mtT1B. Synthetic RNAs produced from both of the mutation-containing plasmids and control plasmids were transfected into Huh-7.5.1 cells. After the transfection, core proteins were secreted into the culture medium at levels similar to those of JFH-1 RNA-transfected cells but at lower levels than J6/JFH1 RNA-transfected cells (Fig. 9A). HCV RNA levels in the culture medium of J6/JFH2/AS/mtT1A (mtT1A) and J6/JFH2/AS/mtT1B (mtT1B) RNA-transfected cells were less than those in cells transfected with either or JFH-1 J6/JFH1 RNA (Fig. 9B). This discrepancy may be due to the lower detection efficiency of the JFH-1 core protein in the immunoassay, as reported previously (31). Infectivity in the culture medium was also determined. Interestingly, higher infectious titers were detected in the culture medium of the J6/JFH2/AS/mtT1A and J6/JFH2/AS/mtT1B

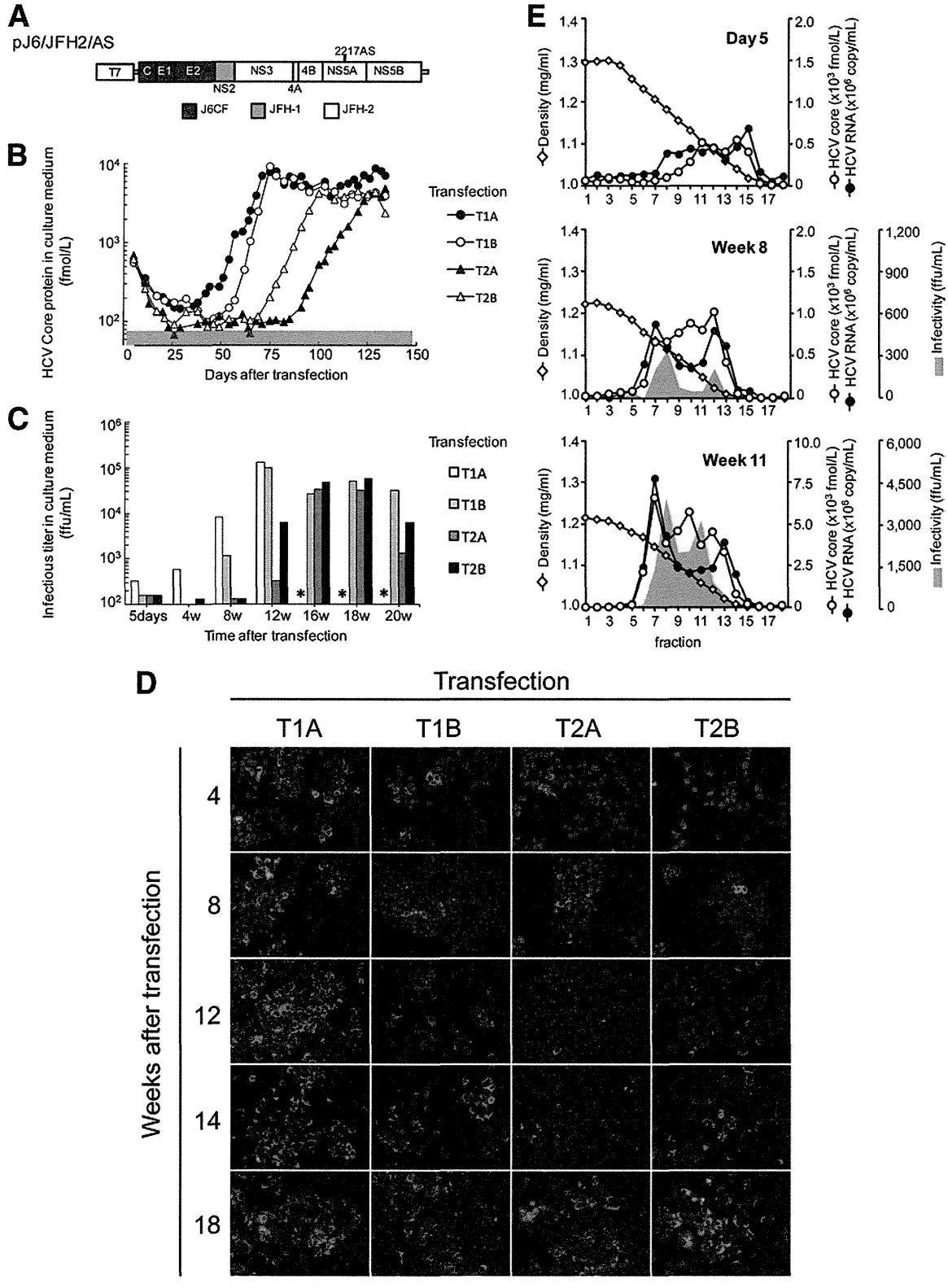

FIG 6 J6/JFH2 chimeric full-length HCV replication. (A) Organization of full-length chimeric JFH-2 construct, pJ6/JFH2/AS. A T7 RNA promoter is located upstream of the 5′ end of the HCV cDNA construct. The 5′ UTR and NS2 region are derived from the JFH-1 strain. Regions of the core protein to E2/p7 are derived from the J6CF strain. The 2217AS adaptive mutation is introduced. (B) Huh-7.5.1 cells were transfected with the transcribed RNA from pJ6/JFH2/AS. Two independently transfected cell lines (transfections 1 and 2 [T1 and T2, respectively]) were divided into two passages, resulting in four independently passaged transfected cell lines (T1A, T1B, T2A, and T2B). At each time point, culture medium was harvested and analyzed for the presence of HCV core protein by Lumipulse Ortho HCV Ag (Ortho-Clinical Diagnostics). The gray area indicates values that are below the detection limit. (C) Infectious titers in the culture supernatant of the passaged transfected cells (T1A, T1B, T2A, and T2B) were determined by focus formation assay. After 16 weeks, the culture media from T1A

TABLE 4 Specific infectivity of culture medium after transfection of J6/JFH2/AS RNA

Cell culture medium (no. of days posttransfection)	Infectivity (FFU/ml)	HCV core protein (fmol/liter)	HCV RNA (no. of copies/ml)	Specific infectivity	
				Infectivity/HCV core protein	Infectivity/HCV RNA (10^4)
T1A (5)	3.20E+1	3.57E+2	2.63E+6	0.09	0.12
T1B (5)	1.60E+1	3.07E+2	2.35E+6	0.05	0.07
T2A (5)	1.60E+1	3.13E+2	2.99E+6	0.05	0.05
T2B (5)	1.60E+1	2.63E+2	3.42E+6	0.06	0.05
T1A (82)	1.28E+4	5.47E+3	2.63E+7	2.34	4.87
T1B (82)	9.83E+3	5.98E+3	2.73E+7	1.64	3.61
T2A (120)	3.17E+3	2.47E+3	8.49E+6	1.28	3.73
T2B (120)	5.83E+3	4.51E+3	2.83E+7	1.29	2.06

RNA-transfected cells than in JFH-1 RNA-transfected cells; however, they were lower than in J6/JFH-1 RNA-transfected cells (Fig. 9C).

Transfected cells were serially passaged, and, importantly, both types of transfected cells (J6/JFH2/AS/mtT1A and J6/JFH2/AS/mtT1B RNA) secreted core protein and HCV RNA at high levels, even at the first passage after transfection, and the levels of HCV core protein and RNA were maintained during the passages (Fig. 10A and B). Infectious titers in the medium of the transfected cells were also measured (Fig. 10C). J6/JFH2/AS/mtT1A secreted a higher infectious titer than J6/JFH2/AS/mtT1B although their HCV core protein levels and RNA levels in the culture medium were similar. To confirm the rapid infectious viral production phenotype of these viruses, we inoculated naive Huh-7.5.1 cells with the culture medium of J6/JFH2/AS/mtT1A and J6/JFH2/AS/mtT1B RNA-transfected cells at 8 and 38 days posttransfection at an MOI of 0.01. All of the inoculated cells secreted core protein and HCV RNA with similar kinetics (Fig. 11A and B). The infectious titer was also determined in the culture medium of the infected and passaged cells (Fig. 11C). mtT1B (day 38 posttransfection) showed lower infectivity at 7 days after inoculation; however, substantial infectivity was detected at 13 and 27 days. The culture medium of mtT1A (day 8 and day 38 posttransfection) was harvested at 20 days after inoculation and analyzed by a sucrose density gradient assay, as described above (Fig. 11D). Major peaks of both HCV core protein and RNA were clearly shown at around 1.15 mg/ml, and the subpeaks of HCV core protein were found in lighter fractions. On the other hand, major peaks of infectivity were found at around 1.0 mg/ml. Compared to the data shown in Fig. 6E, the HCV core and RNA levels and infectivity titer are higher in mtT1A (day 8 and day 38 posttransfection) virus. The similar virus characteristics suggested that J6/JFH2/AS/mtT1A and J6/JFH2/AS/mtT1B viruses do not need further adaptations for autonomous expansion in cultured cells. Thus, we established stable cell culture-adapted virus and constructed recombinant cell culture-adapted infectious HCV clones by reverse genetics.

Human hepatocyte-transplanted uPA/SCID mouse experiment. To determine the *in vivo* infectivity of J6/JFH2/AS virus, we inoculated day 75 culture medium of T1B cells containing 1×10^6 RNA copies of purified J6/JFH2/AS HCV particles and original patient serum also containing 1×10^6 RNA copies into human hepatocyte-transplanted uPA/SCID mice. Inoculation of 1×10^6 RNA copies of cell culture-derived J6/JFH1 virus usually results in robust infection for human hepatocyte-transplanted uPA/SCID mice. Two mice were used for each type of inoculum. Human albumin levels in sera of the inoculated mice were more than 3 mg/ml during the experiment, which supported the high replacement ratio of the human hepatocytes in the mouse liver. Both mice inoculated with patient serum became HCV RNA positive 1 week postinoculation and remained positive during the 4-month observation period (Fig. 12). However, the mice inoculated with J6/JFH2/AS virus in culture medium did not become HCV positive after inoculation (Fig. 12). One mouse inoculated with J6/JFH2/AS virus died 16 days after inoculation, and the cause of death was unknown. HCV RNA was not detected at 7, 14, and 16 days postinoculation. The other mouse inoculated with culture medium was also tested every week for serum HCV RNA and remained negative for 56 days after infection. On day 56, this mouse received a second inoculation with the same culture medium. This mouse was monitored for a total of 63 days, but weekly tests for HCV RNA were continuously negative. Thus, the cell culture-adapted virus in the inoculum may be less viable *in vivo* although the virus acquired robust replication capacity in HuH-7 cells.

Full-length JFH-2 construct. We successfully established J6/JFH2/AS-derived cell culture-adapted viruses. Next, we produced a full-length JFH2/AS virus by using the structural region sequence from JFH-2. pJFH2/AS was constructed according to the viral sequence, and an alanine-to-serine mutation was introduced at amino acid position 2217. JFH2/AS RNA synthesized *in vitro* was electroporated into the Huh-7.5.1 cells, as described above. J6/JFH2/AS RNA was also transfected simultaneously and compared. Two groups of independently transfected cells (transfections 3 and 4 [T3 and T4, respectively]) were analyzed for JFH2/AS and J6/JFH2/AS. Interestingly, JFH2/AS RNA-transfected cells be-

cell lines were not tested (*). (D) The passaged transfected cells were stained with anti-core protein monoclonal antibody (2H9) as a primary antibody at the indicated time points. Green, HCV core protein; blue, 4′,6′-diamidino-2-phenylindole (DAPI) staining. (E) Density gradient analysis of culture supernatant from HCV RNA-transfected Huh-7.5.1 cells. Culture supernatants of transfected cell line T1A collected at 5 days, 8 weeks, and 11 weeks posttransfection were cleared by centrifugation and filtration. Each supernatant was overlaid on the stepwise sucrose density gradient (0%, 10%, 20%, 30%, 40%, 50%, and 60% sucrose) and centrifuged for 16 h at 200,000 × *g* at 4°C. Eighteen fractions were collected from the bottom of the tubes, and the concentration of HCV core protein in each fraction was determined by Lumipulse Ortho HCV Ag. The levels of HCV core protein, HCV RNA, and infectivity were determined in each fraction. Infectivity of the samples from day 5 was negative. Open diamond, buoyant density.

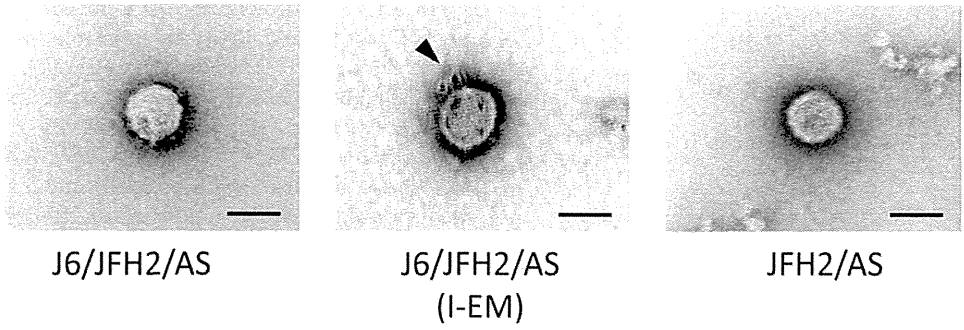

FIG 7 Morphology of JFH-2 virus particles. Negatively stained HCV particles were observed by electron microscopy. J6/JFH-2/AS and JFH2/AS virus particles were purified and observed by electron microscopy by using negative staining. In the middle panel, a J6/JFH-2/AS virus particle was detected by immuno-electron microscopic (I-EM) analysis by using anti-E2 antibody. Arrowhead, gold-labeled antibody. Scale bar, 50 nm.

gan to secrete core proteins earlier than J6/JFH2/AS RNA-transfected cells in this experiment (Fig. 13). Core protein levels were 24,525 and 11,720 fmol/liter in T3 cells at 67 days posttransfection and T4 cells at 63 days posttransfection, respectively. Infectious titers were also determined in the same culture medium at 2.1×10^4 and 4.3×10^4 focus-forming units (FFU)/ml for T3 and T4, respectively. T3 culture medium at day 67 posttransfection was

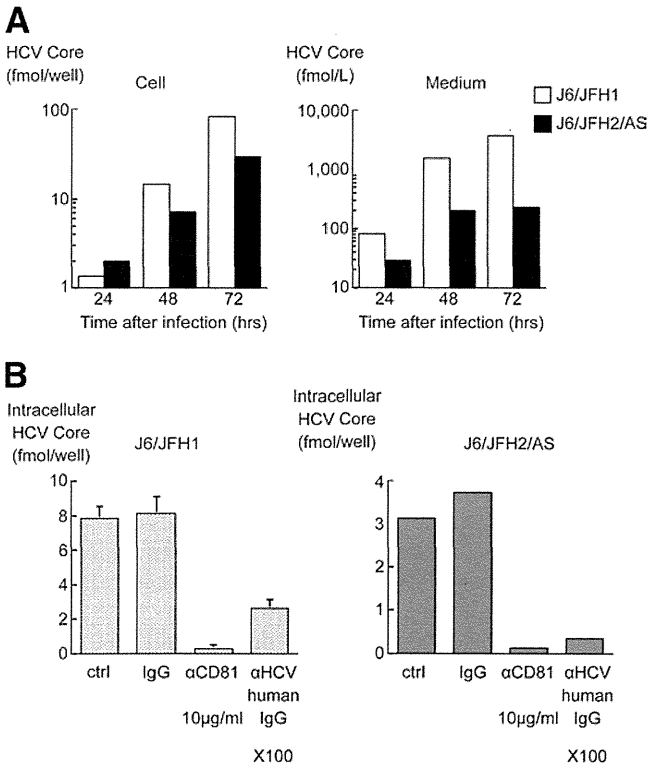

FIG 8 Comparative analysis between J6/JFH1 and J6/JFH2/AS virus. (A) Huh-7.5.1 cells were infected with J6/JFH1 or J6/JFH2/AS virus particles at an MOI of 0.03. HCV core protein production in the inoculated cell lysate and medium was measured at the indicated times. Assays were performed in duplicate, and the average data are represented. (B) Infection with J6/JFH1 and J6/JFH2/AS virus particles was inhibited by adding antibodies to the reaction mixtures. Assays were performed three times independently, and data are presented as means ± standard deviations. Normal human IgG and anti-CD81 monoclonal antibody and anti-HCV human IgG at the indicated concentrations were used. Ctrl, control.

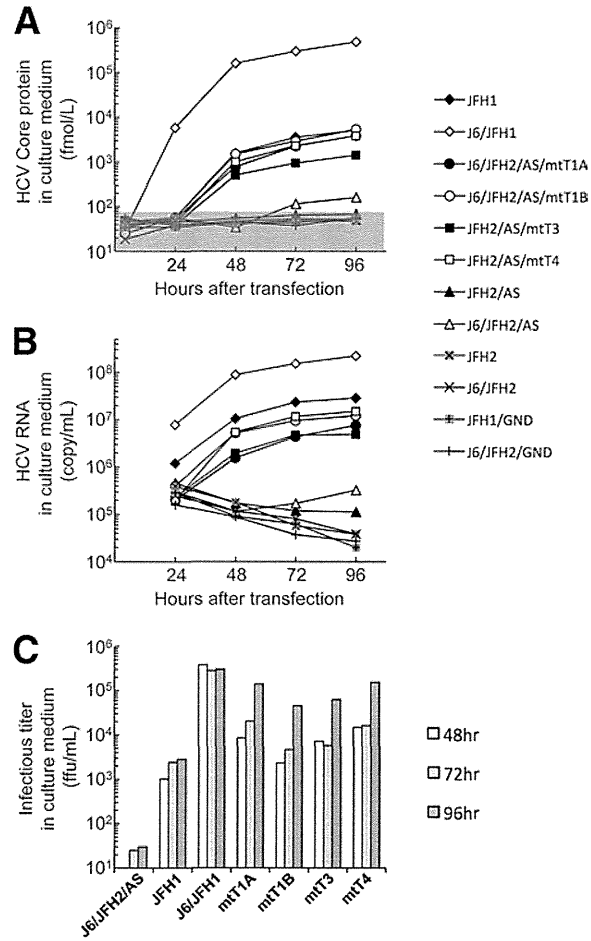

FIG 9 Transient virus production assay of J6/JFH2- and JFH2-related constructs with Huh-7.5.1 cells. Full-length HCV RNA was synthesized from the JFH1, J6/JFH1, JFH2, and J6/JFH2 constructs and their derivatives with mutations and transfected into Huh-7.5.1 cells. (A) HCV core protein levels in the culture medium were determined at 4, 24, 48, 72, and 96 h after transfection. The gray area indicates values that are below the detection limit. (B) HCV RNA levels in the culture medium were also determined at 24, 48, 72, and 96 h after transfection. (C) Infectivity in the culture medium was determined by focus formation assay at 48, 72, and 96 h after transfection. Only positively detected data are shown in the figure. All assays in this figure were performed in duplicate, and the average data are represented.

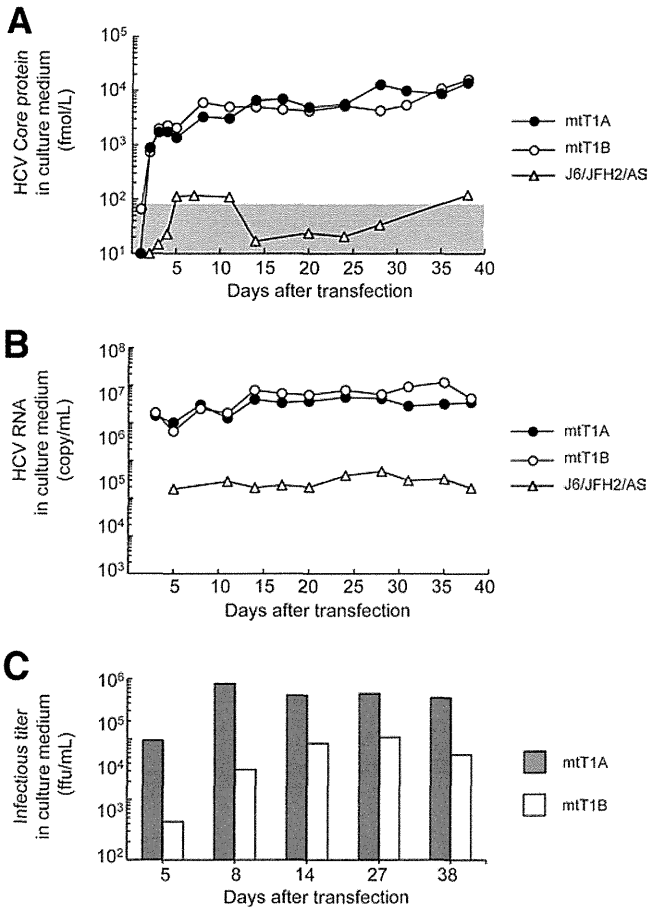

FIG 10 Continuous passage of J6/JFH2/AS cell culture-adapted virus RNA-transfected cells. Full-length HCV RNA was synthesized from the J6/JFH2/AS, J6/JFH2/AS/mtT1A (mtT1A), and J6/JFH2/AS/mtT1B (mtT1B) constructs. RNA-transfected cells were serially passaged until 38 days after transfection, and culture supernatants were harvested at the indicated time points. HCV core protein (A) and HCV RNA (B) levels in the culture media were determined. The data in the gray area were below the detection limit of the assay to detect HCV core protein. (C) Infectivity in the culture medium was determined by focus formation assay at 5, 8, 14, 27, and 38 days after transfection.

also used for electron microscopy analysis. After the density gradient purification, spherical viral particles were detected (Fig. 7, right panel). After the core protein levels plateaued, naive Huh-7.5.1 cells were inoculated with the culture medium, as described above. When the core protein levels plateaued again after the third inoculation of T3 and T4 cells, we sequenced the viral genome in the culture medium (T3i3 and T4i3, respectively) to determine the adaptive mutation. We found the following nonsynonymous mutations: 414IT in E2, 1510EG and 1617RQ in NS3, 2006KQ, 2233AV and 2234NS in NS5A, and 2695TI in NS5B of T3i3; and 387VG in E1, 828VA in NS2, 1225RQ and 1283RG in NS3, 1883VA in NS4B, 2206SA, 2279KN, and 2441CR in NS5A, and 2695TI in NS5B of T4i3 (Fig. 3B). We introduced these mutations into the pJFH2/AS plasmid (pJFH2/AS/mtT3 and pJFH2/AS/mtT4). Synthesized RNA from pJFH2/AS/mtT3 and pJFH2/AS/mtT4 and the related control plasmids was transfected into Huh-7.5.1 cells. HCV core protein levels, HCV RNA levels, and infectivity were monitored in the culture medium of the transfected cells until 96 h after transfection (Fig. 9A to C). JFH2/AS/mtT3 (mtT3) and JFH2/AS/mtT4 (mtT4) secreted similar levels of HCV core protein, RNA, and infectious virus with J6/JFH2/AS/mtT1A and J6/JFH2/AS/mtT1B. Although JFH2/AS/mtT3 secreted slightly higher levels of HCV core protein and RNA than JFH2/AS/mtT4, the secreted infectious virus titers were similar for both viruses. JFH2/AS/mtT3 and JFH2/AS/mtT4 RNA-transfected cells were also serially passaged, and the HCV core proteins were secreted immediately after transfection (Fig. 14A). However, JFH2 and JFH2/AS RNA-transfected cells did not secrete significant amounts of HCV core protein into the culture medium. HCV RNA levels in the culture medium of the RNA-transfected cells were at similar levels for JFH2/AS/mtT3 and JFH2/AS/mtT4 (around 10^7 copy/ml) (Fig. 14B). Infectivity was also detected as higher than 10^4 FFU/ml even at 3 days after the RNA transfection, and this level of infectious titer was maintained during the cell passages (Fig. 14C). We also analyzed JFH2/AS/mtT3 and JFH2/AS/mtT4 culture media by density gradient assay (Fig. 14D). The density profiles with HCV core protein and RNA levels and infectious titers in the fractions were basically similar to those of J6/JFH2/AS-adapted viruses (Fig. 6E and 11D). Taken together, the results described in this section indicate infectious virus was also recovered from the full-length JFH-2 construct with the 2217AS mutation.

Mechanistic analysis of adaptive mutations introduced in the J6/JFH2/AS and JFH2/AS cell culture-adapted viruses. To elucidate the mechanisms of adaptive mutations discovered in J6/JFH2/AS and JFH2/AS virus genomes, we transfected JFH-2 and J6/JFH2 constructs along with possible control constructs into Huh7-25 cells (2) (Fig. 15), which are CD81 defective. The transfection of JFH-1 RNA into Huh7-25 cells results in infectious HCV production, but there was no reinfection into Huh7-25 cells because the cell surface expression of CD81 is essential for HCV infection (10). HCV core protein levels were measured in the culture medium and cell lysate to monitor virus particle secretion and intracellular virus genome replication, respectively (Fig. 15A and B). JFH2/AS, JFH2, J6/JFH2, JFH1/GND, and J6/JFH2/GND RNA-transfected cells did not show increased levels of intracellular core protein expression. However, other RNA-transfected cells showed increased intracellular core protein expression. The cellular core protein level was especially increased at 72 and 96 h after transfection with J6/JFH2/AS RNA, which suggests a higher replication efficiency than J6/JFH; however, core protein secretion was not detected with J6/JFH2/AS, which suggests defective virus particle formation or secretion. Other adaptive mutations in J6/JFH2/AS/mtT1A and J6/JFH2/AS/mtT1B further increased virus genome replication and core protein secretion. In the case of JFH2/AS RNA transfection, cellular core protein expression was not detected, suggesting a lower replication efficiency than that of J6/JFH2/AS. This lower replication efficiency of JFH2/AS may be due to the presence of different sequences in the region of core protein to NS2. However, core protein expression in the cell lysate and culture medium was detected with both JFH2/AS/mtT3 and JFH2/AS/mtT4 RNA transfection. Thus, adaptive mutations in mtT3 and mtT4 are necessary to increase viral genome replication and efficient core protein secretion. JFH-1 and J6/JFH-1 had intracellular core protein expression levels that were similar and high. From the intracellular core protein data, it is clear that J6/JFH2/AS/mtT1A, J6/JFH2/AS/mtT1B, JFH2/AS/mtT3, and JFH2/AS/mtT4 constructs obtained higher replication capacities by

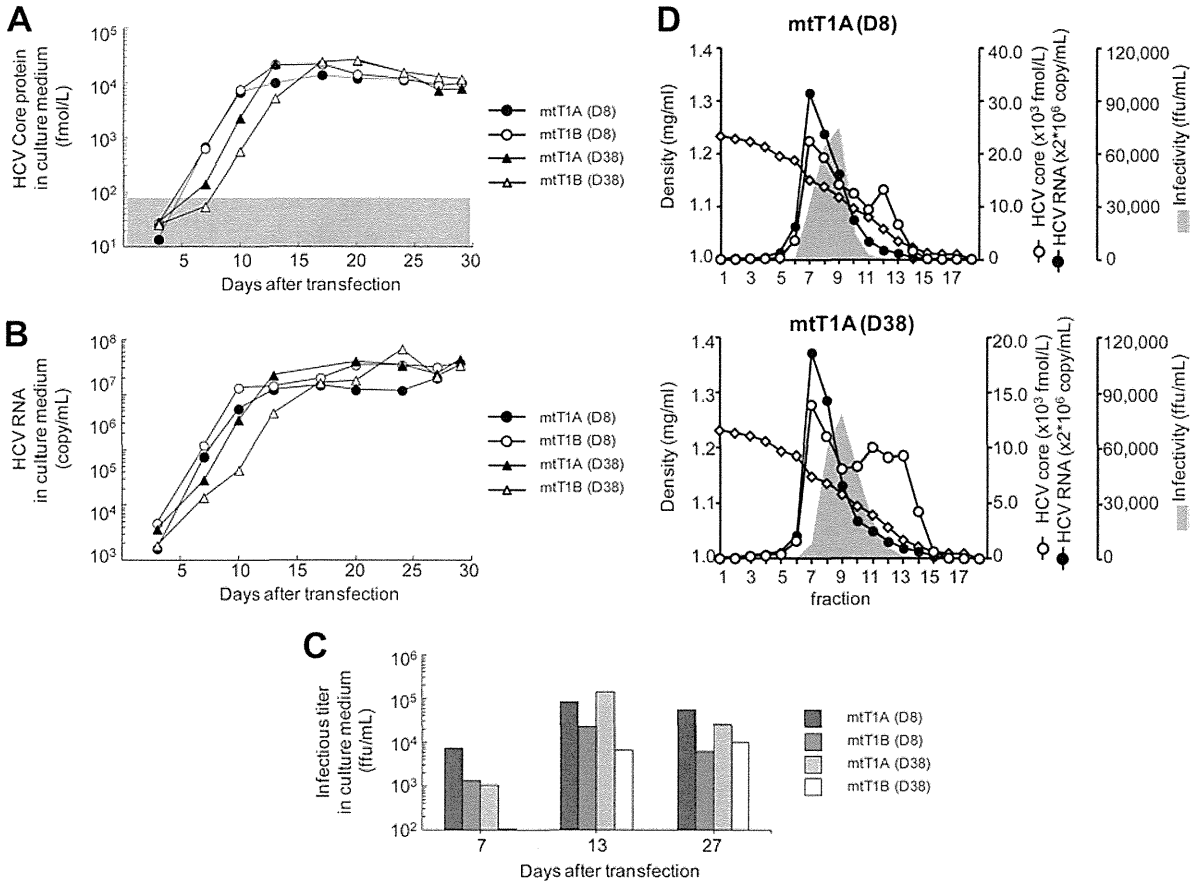

FIG 11 Serial passages of J6/JFH2/AS cell culture-adapted virus infected cells. Naive Huh-7.5.1 cells were inoculated with culture medium of the RNA-transfected cells at an MOI of 0.01. Inoculated cells were serially passaged, and culture supernatants were harvested at the indicated times. HCV core protein (A), HCV RNA (B), and infectivity (C) levels in the culture media were determined. (D) Density gradient analysis of culture supernatant from J6/JFH2/AS/mtT1A cell-culture adapted virus-infected Huh-7.5.1 cells. Culture supernatant of infected Huh-7.5.1 cells with mtT1A (day 8 [D8] D38 posttransfection) was harvested at 20 days after inoculation. Assays were performed as described in the legend of Fig. 6E. Open diamond, buoyant density.

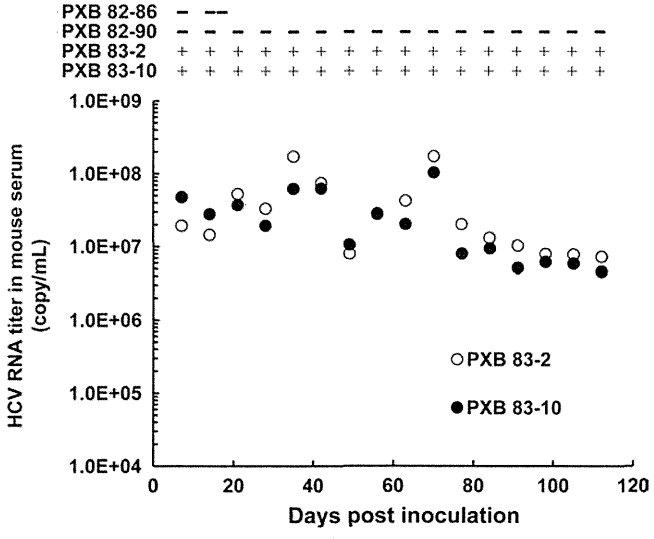

FIG 12 Serum HCV RNA titer in human hepatocyte-transplanted uPA/SCID mice inoculated with JFH-2 serum and cell culture-adapted virus. Mice PXB 82-86 and PXB 82-90 were inoculated with the cell culture-adapted J6/JFH2/AS HCV particles, and mice PXB 83-2 and PXB 83-10 were inoculated with JFH-2 patient serum. Upper and lower panels indicate the results of the RT-PCR and the quantitative detection RT-PCR of HCV RNA in mouse serum, respectively.

adaptive mutations; however, their replication levels are lower than those of JFH-1 and J6/JFH1.

We also analyzed the ratio of extracellular protein to total core protein to analyze the virus secretion efficiency (Fig. 15C). J6/JFH-1 secreted a higher percentage of core protein into culture

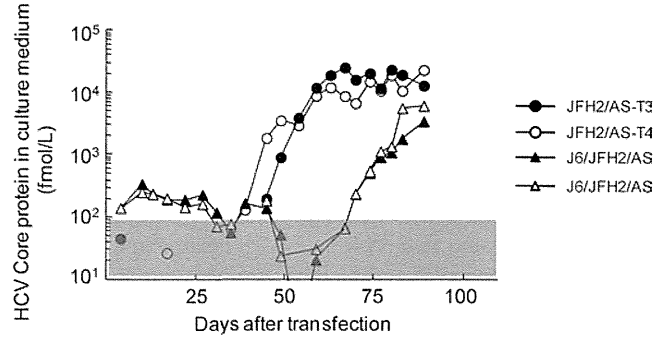

FIG 13 Propagation of a full-length JFH2 virus. Huh-7.5.1 cells were transfected with the transcribed RNA from pJFH2/AS and pJ6/JFH2/AS. Two independently JFH2/AS RNA-transfected cell lines (T3 and T4) were independently passaged. At each time point, culture medium was harvested and analyzed for the presence of HCV core protein.

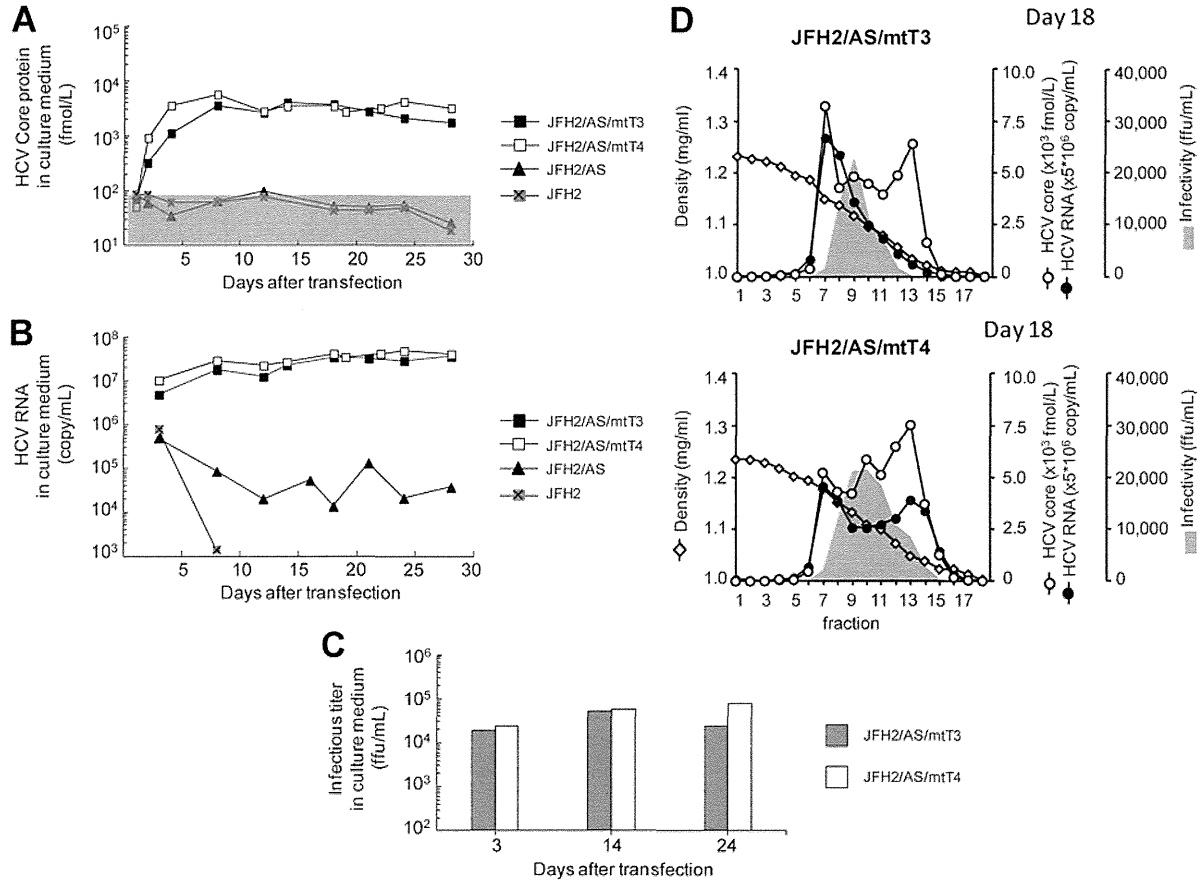

FIG 14 Full-length RNA was synthesized from the JFH2 construct and its derivatives with mutations. RNA-transfected cells were serially passaged, and culture supernatants were harvested at the indicated time points. HCV core protein (A), HCV RNA (B), and infectivity (C) levels in the culture media were determined. The data in the gray area were below the detection limit of the assay to detect HCV core protein. (D) Density gradient analysis of culture supernatant from JFH2/AS cell-culture adapted virus-infected Huh-7.5.1 cells. Culture supernatants of Huh-7.5.1 cells infected with JFH2/mtT3 and JFH2/mtT4 viruses were harvested 18 days after inoculation. Assays were performed as described in the legend of Fig. 6E. Open diamond, buoyant density.

medium than JFH-1. J6/JFH2/AS/mtT1A, J6/JFH2/AS/mtT1B, JFH2/AS/mtT3, and JFH2/AS/mtT4 RNA-transfected cells showed different percentages of secreted core protein. mtT1A and mtT1B constructs showed similar replication levels (Fig. 15B), but mtT1B showed a higher percentage of core protein secretion than mtT1A (Fig. 15C). mtT3 and mtT4 showed similar percentages of core protein secretion, which are higher than the level of JFH1 (Fig. 15C). Because J6/JFH2/AS RNA-transfected cells did not secrete core protein despite intracellular core protein expression (Fig. 15A and B), the adaptive mutant constructs obtained core protein (or virus particle) secretion phenotypes. Thus, during the adaptation process, the viruses obtained both higher replication capacity and core protein secretion capacity by their adaptive mutations.

Other HCV constructs with the 2217AS mutation. The alanine residue at amino acid position 2217 is located in the ISDR of NS5A, and it is conserved among HCV strains including genotype 1 and 2 strains. Because the 2217AS mutation in NS5A is the key mutation for the production of cell culture-adapted HCV, we introduced this mutation into other wild-type HCV constructs, i.e., H77 (genotype 1a), Con1 (genotype 1b), and J6CF (genotype 2a). Synthetic RNAs including the 2217AS mutation were electroporated into Huh-7.5.1 cells, and then the transfected cells were serially passaged. HCV core protein secretion was measured in the culture medium of transfected cells. However, we could not observe the increment of HCV core levels in the culture medium (data not shown). Therefore, we concluded that the 2217AS mutation does not always induce cell culture adaptation in HCV isolates.

DISCUSSION

In previous studies, we have isolated cell culture-infectious HCV, the JFH-1 strain, from a patient with fulminant hepatitis (14, 38). In this report, we isolated another HCV cDNA, named JFH-2, also from a fulminant hepatitis patient. We constructed a subgenomic replicon with the JFH-2 sequence, but its replication efficiency was low. Among the mutations found in the replicon genome, the 2217AS mutation in the ISDR exhibited the strongest adaptive effect. Interestingly, the full-length chimeric or wild-type JFH-2 genome with adaptive mutations could replicate and produce infectious virus particles. Virus infection efficiency was sufficient for autonomous virus propagation in cultured cells.

Several full-length HCV cDNAs have been cloned, and their infectivity has been confirmed *in vivo* with chimpanzee models (18, 39). However, it has been difficult to produce recombinant viral particles and test their infectivity by using cell culture

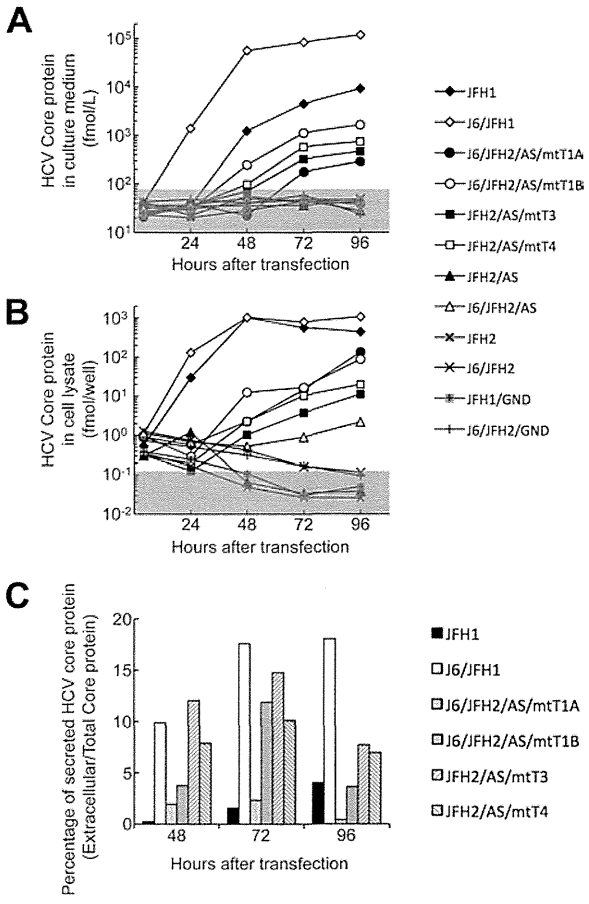

FIG 15 Transient virus production assay of J6/JFH2- and JFH2-related constructs with CD81-defective Huh7-25 cells. Full-length HCV RNA was synthesized from the JFH1, J6/JFH1, JFH2, and J6/JFH2 constructs and their derivatives with mutations and transfected into Huh7-25 cells. (A) HCV core protein levels in culture medium were determined at 4, 24, 48, 72, and 96 h after transfection. The data in the gray area were below detection limit. (B) HCV core protein levels in the cell lysate were determined at 24, 48, 72, and 96 h after transfection. (C) Percentages of secreted HCV core protein from the transfected cells were determined at 48, 72, and 96 h after transfection. Percentages of secreted HCV core protein were calculated only for the indicated viruses. All assays were performed in duplicate, and the data represent average values.

systems (4, 28). Only the JFH-1 strain efficiently replicates in HuH-7 cells and other hepatic and nonhepatic cell lines in subgenomic replicon form (20, 38, 41). Full-length wild-type JFH-1 RNA and chimeric JFH-1 RNA can replicate in HuH-7 cells and produce infectious virus. Since the JFH-1 strain was isolated from a patient with fulminant hepatitis, we assumed that virus strains that cause fulminant hepatitis may replicate efficiently in cultured cells. To identify more HCV clones that can replicate in cultured cells, we isolated the JFH-2 strain from another fulminant hepatitis patient (15). Interestingly, the JFH-2 strain showed a low level of replication in cultured cells in the initial subgenomic replicon experiment. This result may suggest that HCV strains isolated from fulminant hepatitis patients are able to replicate more efficiently than strains from chronic hepatitis patients; however, this hypothesis should be confirmed by testing more HCV strains from patients with fulminant hepatitis. The JFH-2 patient received a course of betamethasone therapy and developed fulminant hepatitis after the withdrawal of betamethasone. It is thus possible that the JFH-2 strain obtained its higher replication capacity in the immune-suppressed host environment. To confirm this hypothesis, we must test the replication efficiency of HCV strains isolated from other immune-suppressed patients, such as patients who are coinfected with HIV, patients who are reinfected after a transplant, and patients who are treated with immunosuppressive agents.

In previous reports, adaptive mutations have been found to enhance viral RNA replication at the expense of virus particle formation efficiency (28). A highly cell culture-adapted Con1 strain can replicate in cultured cells, but it cannot produce infectious virus particles. Interestingly, a highly adapted Con1 strain was not infectious for chimpanzees, while moderately adapted Con1 was infectious. However, the virus recovered from the infected animal was wild-type Con1 virus (5). This result clearly suggests that HCV strains with lower replication efficiencies are favorable for *in vivo* infection. However, we must note that the "replication efficiency" is determined in cultured cells. In the case of JFH-2, we found several adaptive mutations in the subgenomic replicon clones, and the most adaptive mutation, 2217AS, was tested in full-length HCV replication and virus production. After the RNA transfection of J6/JFH2/AS, we could not detect substantial virus secretion for about 30 days. However, after 30 days, significant levels of infectious virus particles were secreted into the culture medium. Naive Huh-7.5.1 cells were inoculated three times with the cell culture-adapted virus. This virus adaptation was also tested with full-length JFH2/AS, and we successfully obtained infectious JFH2/AS virus. Both the J6/JFH2/AS and JFH2/AS viruses acquired the ability for autonomous virus expansion in Huh-7.5.1 cells, and several additional mutations were found in their genomes. Interestingly, the 2695TI mutation in NS5B was commonly found in all of the adapted virus genomes, and isoleucine at amino acid position 2695 is also found in the JFH-1 strain. However, the introduction of only the 2695TI mutation into the J6/JFH2/AS or JFH2/AS virus genome did not restore robust virus production (data not shown). After repeated virus passages, mutations were found throughout the viral genome (in J6/JFH2/AS-T1Ai3 and -T1Bi3 and in JFH2/AS-T3i3 and -T4i3), and we are currently investigating which mutations or combinations of mutations are most important for this adaptation. From the comparisons of cell culture-adapted viruses and their parental virus constructs, adaptive mutations are necessary to increase both viral genome replication and virus particle assembly/secretion efficiency (Fig. 15). The procedure to produce cell culture-adapted HCV was thus established. The adaptive mutations found from the subgenomic replicon assay were introduced into the full-length genome, and the cells transfected with virus RNA were repeatedly passaged until the virus particles were produced.

In vivo infectivity may be inversely related to the replication efficiency in cultured cells, as discussed above. The original JFH-2 patient serum was infectious in human liver-transplanted mice; however, cell culture-adapted J6/JFH2/AS virus was not infectious. The JFH-1 virus was infectious not only for cultured cells but also for chimpanzees and human liver-transplanted mice (10, 38). However, the JFH-1 infection in chimpanzees was only mild and transient without any liver pathology. Thus, the J6/JFH2/AS and JFH2/AS viruses are more cell culture-adapted and attenuated than the JFH-1 virus. It may be worthwhile to test this cell culture-

adapted strain as a live attenuated vaccine candidate to induce protective immunity. However, for ethical reasons, the necessary chimpanzee experiments are not appropriate to perform. Therefore, we should wait for the establishment of immunocompetent small-animal models susceptible to HCV infection to perform this kind of study. Furthermore, future studies should examine the *in vivo* infectivity of the adapted J6/JFH2 and JFH2 viruses isolated in the present study.

The 2217AS mutation is located in the ISDR. In the previous study of the genotype 1b subgenomic replicon, mutations introduced into the ISDR enhanced the colony formation efficiency of the HCV replicons (17, 23). However, mutations in the ISDR impaired the genotype 1b HCV replication in human liver-transplanted mice (9). The exact mechanism of the ISDR is still not clear although the number of mutations in the ISDR is related to the efficacy of interferon therapy (8). Our results in this study also support the concept that the 2217AS mutation in the ISDR enhances replicon replication efficiency although the J6/JFH2/AS virus did not infect human liver-transplanted mice. Further studies are necessary to understand the molecular mechanism of the effects of adaptive mutations in the ISDR.

In the present study, we established a cell culture-adapted HCV strain, JFH-2. The virus could be passaged continuously in naive Huh-7.5.1 cells. This approach may be applicable to the establishment of new infectious HCV clones. Novel antiviral drugs are under development, and some of them will be used in the clinical setting. However, most of them target genotype 1 HCV strains. To eradicate other genotypes of HCV, it is important to establish their replicons and infectious virus culture systems.

ACKNOWLEDGMENTS

Huh-7.5.1 cells were kindly provided by Francis V. Chisari. The J6CF plasmid was a kind gift from Jens Bukh. Anti-HCV human IgG was a kind gift from Hiroshi Yoshizawa and Junko Tanaka, Hiroshima University. AP33 antibody was generously provided by Genentec. We thank Tetsuro Suzuki and Hideki Aizaki for their helpful discussions. We also thank Minako Kaga for her technical assistance.

This work was partially supported by Grants-in-Aid for Scientific Research from the Japan Society for the Promotion of Science, from the Ministry of Health, Labor and Welfare of Japan, from the Ministry of Education, Culture, Sports, Science and Technology, from the National Institute of Biomedical Innovation, and by the Research on Health Sciences Focusing on Drug Innovation from the Japan Health Sciences Foundation.

REFERENCES

1. **Aizaki H, et al.** 2008. Critical role of virion-associated cholesterol and sphingolipid in hepatitis C virus infection. J. Virol. **82**:5715–5724.
2. **Akazawa D, et al.** 2007. CD81 expression is important for the permissiveness of Huh7 cell clones for heterogeneous hepatitis C virus infection. J. Virol. **81**:5036–5045.
3. **Akazawa D, et al.** 2011. Production and characterization of HCV particles from serum-free culture. Vaccine **29**:4821–4828.
4. **Bartenschlager R, Lohmann V.** 2000. Replication of hepatitis C virus. J. Gen. Virol. **81**:1631–1648.
5. **Bukh J, et al.** 2002. Mutations that permit efficient replication of hepatitis C virus RNA in Huh-7 cells prevent productive replication in chimpanzees. Proc. Natl. Acad. Sci. U. S. A. **99**:14416–14421.
6. **Choo QL, et al.** 1989. Isolation of a cDNA clone derived from a blood-borne non-A non-B viral hepatitis genome. Science **244**:359–362.
7. **Di Bisceglie AM, Hoofnagle JH.** 2002. Optimal therapy of hepatitis C. Hepatology **36**:S121–S127.
8. **Enomoto N, et al.** 1995. Sensitivity to interferon is conferred by amino acid substitutions in the NS5A region. J. Clin. Invest. **96**:224–230.
9. **Hiraga N, et al.** 2011. Impact of viral amino acid substitutions and host interleukin-28b polymorphism on replication and susceptibility to interferon of hepatitis C virus. Hepatology **54**:764–771.
10. **Kato T, et al.** 2008. Hepatitis C virus JFH-1 strain infection in chimpanzees is associated with low pathogenicity and emergence of an adaptive mutation. Hepatology **48**:732–740.
11. **Kato T, et al.** 2003. Efficient replication of the genotype 2a hepatitis C virus subgenomic replicon. Gastroenterology **125**:1808–1817.
12. **Kato T, et al.** 2005. Detection of anti-hepatitis C virus effects of interferon and ribavirin by a sensitive replicon system. J. Clin. Microbiol. **43**:5679–5684.
13. **Kato T, et al.** 2006. Cell culture and infection system for hepatitis C virus. Nat. Protoc. **1**:2334–2339.
14. **Kato T, et al.** 2001. Sequence analysis of hepatitis C virus isolated from a fulminant hepatitis patient. J. Med. Virol. **64**:334–339.
15. **Kato T, et al.** 2003. Processing of hepatitis C virus core protein is regulated by its C-terminal sequence. J. Med. Virol. **69**:357–366.
16. **Kiyosawa K, et al.** 1990. Interrelationship of blood transfusion, non-A, non-B hepatitis and hepatocellular carcinoma: analysis by detection of antibody to hepatitis C virus. Hepatology **12**:671–675.
17. **Kohashi T, et al.** 2006. Site-specific mutation of the interferon sensitivity-determining region (ISDR) modulates hepatitis C virus replication. J. Viral Hepat. **13**:582–590.
18. **Kolykhalov AA, et al.** 1997. Transmission of hepatitis C by intrahepatic inoculation with transcribed RNA. Science **277**:570–574.
19. **Kuo G, et al.** 1989. An assay for circulating antibodies to a major etiologic virus of human non-A non-B hepatitis. Science **244**:362–364.
20. **Lindenbach BD, et al.** 2005. Complete replication of hepatitis C virus in cell culture. Science **309**:623–626.
21. **Lindenbach BD, et al.** 2006. Cell culture-grown hepatitis C virus is infectious in vivo and can be recultured in vitro. Proc. Natl. Acad. Sci. U. S. A. **103**:3805–3809.
22. **Lohmann V, et al.** 1999. Replication of subgenomic hepatitis C virus RNAs in a hepatoma cell line. Science **285**:110–113.
23. **Maekawa S, et al.** 2004. Introduction of NS5A mutations enables subgenomic HCV replicon derived from chimpanzee-infectious HC-J4 isolate to replicate efficiently in Huh-7 cells. J. Viral Hepat. **11**:394–403.
24. **McHutchison JG, et al.** 1998. Interferon alfa-2b alone or in combination with ribavirin as initial treatment for chronic hepatitis C. N. Engl. J. Med. **339**:1485–1492.
25. **Merck & Co.** 2011. Victrelis (boceprevir) prescribing information. Merck & Co., Whitehouse Station, NJ. http://www.accessdata.fda.gov/drugsatfda_docs/label/2011/202258lbl.pdf.
26. **Murayama A, et al.** 2007. The NS3 helicase and NS5B-to-3′X regions are important for efficient hepatitis C virus strain JFH-1 replication in Huh7 cells. J. Virol. **81**:8030–8040.
27. **Murayama A, et al.** 2010. RNA polymerase activity and specific RNA structure are required for efficient HCV replication in cultured cells. PLoS Pathog. **6**:e1000885. doi:10.1371/journal.ppat.1000885.
28. **Pietschmann T, et al.** 2002. Persistent and transient replication of full-length hepatitis C virus genomes in cell culture. J. Virol. **76**:4008–4021.
29. **Pietschmann T, et al.** 2009. Production of infectious genotype 1b virus particles in cell culture and impairment by replication enhancing mutations. PLoS Pathog. **5**:e1000475. doi:10.1371/journal.ppat.1000475.
30. **Poynard T, et al.** 1998. Randomised trial of interferon α2b plus ribavirin for 48 weeks or for 24 weeks versus interferon α2b plus placebo for 48 weeks for treatment of chronic infection with hepatitis C virus. Lancet **352**:1426–1432.
31. **Saeed M, et al.** 2009. Evaluation of hepatitis C virus core antigen assays in detecting recombinant viral antigens of various genotypes. J. Clin. Microbiol. **47**:4141–4143.
32. **Takahashi H, et al.** 2010. Biological properties of purified recombinant HCV particles with an epitope-tagged envelope. Biochem. Biophys. Res. Commun. **395**:565–571.
33. **Tateno C, et al.** 2004. Near completely humanized liver in mice shows human-type metabolic responses to drugs. Am. J. Pathol. **165**:901–912.
34. **U. S. Food and Drug Administration.** 2011. FDA news release. FDA approves Incivek for hepatitis C. U.S. Food and Drug Administration, Silver Spring, MD. http://www.fda.gov/NewsEvents/Newsroom/PressAnnouncements/ucm256299.htm.
35. **U. S. Food and Drug Administration.** 2011. FDA news release. FDA approves Victrelis for hepatitis C. U.S. Food and Drug Administration,

Silver Spring, MD. http://www.fda.gov/NewsEvents/Newsroom/PressAnnouncements/ucm255390.htm.
36. **Vertex Pharmaceuticals.** 2011. Incivek (telaprevir) prescribing information. Vertex Pharmaceuticals, Cambridge, MA. http://www.accessdata.fda.gov/drugsatfda_docs/label/2011/201917lbl.pdf.
37. **Wakita T.** 2009. Isolation of JFH-1 strain and development of an HCV infection system. Methods Mol. Biol. **510**:305–327.
38. **Wakita T, et al.** 2005. Production of infectious hepatitis C virus in tissue culture from a cloned viral genome. Nat. Med. **11**:791–796.
39. **Yanagi M, Purcell RH, Emerson SU, Bukh J.** 1997. Transcripts from a single full-length cDNA clone of hepatitis C virus are infectious when directly transfected into the liver of a chimpanzee. Proc. Natl. Acad. Sci. U. S. A. **94**:8738–8743.
40. **Yanagi M, Purcell RH, Emerson SU, Bukh J.** 1999. Hepatitis C virus: an infectious molecular clone of a second major genotype (2a) and lack of viability of intertypic 1a and 2a chimeras. Virology **262**:250–263.
41. **Zhong JP, et al.** 2005. Robust hepatitis C virus infection in vitro. Proc. Natl. Acad. Sci. U. S. A. **102**:9294–9299.

aptara | MIM | mim'437 | Dispatch: March 16, 2012 | CE: N/A
Journal | MSP No. | No. of pages: 10 | PE: Helen

Microbiol Immunol 2012; **00**: 1–10
doi:10.1111/j.1348-0421.2012.00437.x

ORIGINAL ARTICLE

Replication and infectivity of a novel genotype 1b hepatitis C virus clone

Tomoko Date[1], Kenichi Morikawa[1,2,†], Yasuhito Tanaka[3], Keiko Tanaka-Kaneko[4], Tetsutaro Sata[4,‡], Masashi Mizokami[5] and Takaji Wakita[1]

Departments of [1]Virology II and [4]Pathology, National Institute of Infectious Diseases, 1-23-1 Toyama, Shinjuku, Tokyo 162-8640, [2]Division of Gastroenterology, Department of Medicine, Showa University School of Medicine, 1-5-8 Hatanodai, Shinagawa-ku, Tokyo 142-8666, [3]Department of Virology & Liver Unit, Nagoya City University Graduate School of Medical Sciences, Kawasumi, Mizuho, Nagoya 467-8601, and [5]The Research Center for Hepatitis and Immunology, National Center for Global Health and Medicine, 1-7-1 Kounodai, Ichikawa 272-8516, Japan

ABSTRACT

Hepatitis C virus infection is a major public health problem because of an estimated 170 million carriers worldwide. Genotype 1b is the major subtype of HCV in many countries and is resistant to interferon therapy. Study of the viral life cycle is important for understanding the mechanisms of interferon resistance of genotype 1b HCV strains. For such studies, genotype 1b HCV strains that can replicate and produce infectious virus particles in cultured cells are required. In the present study, we isolated HCV cDNA, which we named the NC1 strain, from a patient with acute severe hepatitis. Subgenomic replicon experiments revealed that several mutations enhanced the colony-formation efficiency of the NC1 replicon. The full-length NC1 genome with these adaptive mutations could replicate in cultured cells and produce infectious virus particles. The density gradient profile and morphology of the secreted virus particles were similar to those reported for the JFH-1 virus. Further introduction of a combination of mutations of the NS3 and NS5a regions into the NC1 mutants further enhanced secreted core protein levels and infectious virus titers in the culture medium of HCV-RNA-transfected cells. However, the virus infection efficiency was not sufficient for autonomous virus propagation in cultured cells. In conclusion, we established a novel cell culture-adapted genotype 1b HCV strain, termed NC1, which can produce infectious virus when the viral RNA is transfected into cells. This system provides an important opportunity for studying the life cycle of the genotype 1b HCV.

Key words genotype 1b, hepatitis C virus (HCV), replicon, virus culture.

Hepatitis C virus infection leads to chronic liver diseases including cirrhosis and hepatocellular carcinoma, and is a major public health problem because of an estimated 170 million carriers worldwide (1–3). HCV is a plus-strand RNA virus that displays marked genetic heterogeneity and is currently classified into six major genotypes (4). Some HCV genotypes display regional distribution, although genotypes 1 and 2 occur worldwide. Genotype 1b is the major subtype in Japan, whereas genotype 2a is the most common minor subtype (5). Infection with genotype 1b HCV is known to be resistant to interferon therapy, whereas infection with genotype 2a is

Correspondence
Takaji Wakita, Second Department of Virology, National Institute of Infectious Diseases, 1-23-1 Toyama, Shinjuku-ku, Tokyo 162-8640, Japan.
Tel: +81 3 5285 1111; fax: +81 3-5285 1161; email: wakita@nih.go.jp
Present addresses
[†]Division of Gastroenterology and Hepatology, Centre Hospitalier Universitaire Vaudois, University of Lausanne, Lausanne, Switzerland.
[‡]Toyama Institute of Health, Toyama, Japan.

Received 19 January 2012; revised 23 January 2012; accepted 26 January 2012.

List of Abbreviations: CFU, colony-forming units; DMEM, Dulbecco's modified Eagle's medium; EMCV, encephalomyocarditis virus; ffu, focus-forming units; HCV, hepatitis C virus; IFN, interferon; IRES, internal ribosomal entry site; PI, protease inhibitors; RTD-PCR, real-time detection RT-PCR.

usually sensitive to such intervention (6). Current standard therapy for HCV-related chronic hepatitis is based on a combination of IFN and ribavirin, although virus eradication rates are limited to approximately 50% for genotype 1b HCV infection (7–9). PI have been approved for clinical use against HCV infection in the USA, Europe and Japan, and triple combination therapy that includes PI is expected to improve treatment efficacy. However, the development of other anti-HCV drugs with different modes of action is important to achieve greater efficacy and to avoid the emergence of drug-resistant viruses. To that end, a detailed understanding of the viral replication mechanism is needed to identify novel antiviral targets.

Although HCV belongs to the *Flaviviridae* family and has a genome structure similar to the other flaviviruses, efficient virus propagation in cultured cells has been difficult ever since the discovery of the virus (10). A subgenomic HCV-RNA replicon system was developed using the genotype 1b Con1 strain (11), which enabled the assessment of HCV replication in cultured cells. Subsequently, the genotype 2a JFH-1 strain was cloned and a HCV culture system was established using this strain (12–14). However, such efficient virus production could not be reproduced using genotype 1b HCV strains, even when adaptive mutations were introduced to enhance their replication efficiency in cultured cells (15). Thus, it remains necessary to obtain genotype 1b HCV strains that can replicate and produce infectious virus particles in cultured cells.

In the present study, we isolated HCV cDNA, which we named the NC1 strain, from a patient with acute severe hepatitis. In a subgenomic replicon experiment using the NC1 clone, we found several mutations that enhanced colony-formation efficiency of the NC1 replicon. Interestingly, the full-length NC1 genome with these adaptive mutations could replicate in cultured cells and produce infectious virus particles. However, the viral infection efficiency was not sufficient for autonomous virus propagation in cultured cells even though virus production efficiency could be increased by the introduction of multiple mutations into the virus genome.

MATERIALS AND METHODS

Cell culture system

Huh7 and Huh7.5.1 cells (a generous gift from Dr Francis V. Chisari) were cultured in 5% CO_2 at 37°C in DMEM containing 10% fetal bovine serum (DMEM-10) (13, 16).

HCV clones

The genotype 1b HCV clone NC1 was isolated from a patient with acute severe hepatitis (prothrombin time <40%). The patient was a 48-year-old woman who had no history of blood transfusions. Total RNA was extracted from the serum during the acute phase, and HCV cDNA covering the entire genome was amplified by RT-PCR using HCV-specific primers (S-Table 1). All amplified products were purified and then cloned into pGEM-T EASY^{TM} vectors (Promega, Madison, WI, USA). PCR products and plasmids were sequenced using HCV-specific primer sets (S-Table1), a Big Dye Terminator Mix and an automated DNA sequencer (PE Biosystems, Foster City, CA, USA). Based on the consensus sequence of the NC1 strain, we then assembled pNC1 (DDBJ/EMBL/GenBank accession number: AB691953), which contained the full-length NC1 cDNA downstream of the T7 RNA polymerase promoter. An NC-1 subgenomic replicon construct, pSGR-NC1, was also assembled according to previously published methods used for Con1 replicon and pSGR-JFH1 construction (10, 17). The first 213 nucleotides at the NS3 region of pSGR-NC1 are identical with the Con1 sequence because of the restriction site used for plasmid construction. Several mutations were introduced into the pNC1 and pSGR-NC1 constructs as reported previously using specific primer sets (S-Table 2) (17). pNC1/wt contained the wild-type sequence of the NC1 strain. pNC1/SY and pNC1/SG contained S2197Y and S2204G mutations, respectively. pNC1/EGSY contained both E1202G and S2197Y mutations. pNC1/KTSY contained both K1846T and S2197Y mutations. pNC1/EGKTSY contained the three mutations, E1202G, K1846T and S2197Y.

Subgenomic replicon assay

Subgenomic replicon RNA was synthesized as reported previously (17). The synthesized replicon RNA (3 μg) was adjusted to a total RNA amount of 10 μg using cellular RNA isolated from non-transfected Huh7 cells and was then electroporated into naive Huh7 and Huh 7.5.1 cells as reported previously (17). G418 (1 mg/mL) was added to the culture medium for 3 weeks, and drug-resistant colonies were fixed with buffered formalin and stained with crystal violet or were cloned for further analysis. For the cloning analysis of the replicon cells, G418-resistant colonies were isolated by using cloning cylinders (Asahi Techno Glass Co., Tokyo, Japan) and were expanded until they reached 80% to 90% confluency in 10-cm diameter dishes. Total RNA was extracted from the cloned G418-resistant cells by using the ISOGEN reagent (Nippon Gene, Tokyo, Japan), and the replicon RNA was quantified using real-time detection RT-PCR (RTD-PCR) as reported previously (18). The cDNAs of the HCV-RNA replicon were synthesized and then amplified by PCR. The sequence of each replicon was determined (17).

Full-length HCV-RNA transfection

Full-length HCV-RNA was synthesized from pNC1 and its derivatives that contained adaptive mutations as described previously (12, 19, 20). Synthesized HCV-RNA (10 μg) was transfected into Huh7.5.1 cells. The HCV core protein level in the culture supernatant was measured using Lumipulse Ortho HCV Ag (Ortho-Clinical Diagnostics, Tokyo, Japan) (21), and infectivity of the supernatant was determined by measurement of its focus-formation efficiency (13, 19). In some experiments, the transfected cell pellet was harvested and dissolved with RIPA buffer containing 0.1% SDS. HCV core protein levels in cell lysates were also measured using the Lumipulse Ortho HCV Ag.

Density gradient analysis of secreted virus particles

Culture medium (1 mL) derived from transfected cells was harvested for density gradient analysis 2 or 15 days after transfection of full-length NC1/SY HCV RNA. The cleared culture medium was layered onto a stepwise sucrose gradient (60% [wt/vol] to 10%) and centrifuged for 16 hrs in an SW41 rotor (Beckman, Palo Alto, CA, USA) at 200,000 $\times$ g at 4°C. After centrifugation, 18 fractions were harvested from the bottom of the tubes. The core protein concentration in each fraction was determined by analysis of 100 μL of each fraction.

Electron microscopy

Culture medium (150 mL) containing NC1/SY virus particles were collected from the cells 15 days after transfected cells. The collected culture medium was ultrafiltrated and concentrated 20-fold using a pellicon-2 filter system (Millipore, Bedford, MA, USA). The sample was layered onto a stepwise sucrose gradient (60% [wt/vol] to 10%) and centrifuged for 4 hrs in an SW28 rotor (Beckman, Palo Alto, CA, USA) at 140,000 $\times$ g at 4°C. Thereafter, fractions were harvested from the bottom of the tubes. The core protein concentration in each fraction was determined and the fraction with the highest core protein level was ultrafiltrated for electron microscopic analysis. To visualize HCV particles, we adsorbed the purified virus samples onto carbon-coated grids for 1 min. The grids were then stained with 1% uranyl acetate for 1 min and examined under an H-7650 transmission electron microscope (Hitachi High-Technologies Co., Tokyo, Japan) (22).

Human hepatocyte chimeric mice experiments

Human hepatocytes were transplanted into uPA$^{+/+}$/SCID$^{+/+}$ mice as described previously (23, 24). These mice were obtained from Phoenix Bio Co., Ltd (Hiroshima, Japan). All mice received hepatocyte transplants from the same donor. Human albumin levels in the sera of the mice were monitored to evaluate the percentage replacement of mouse hepatocytes with human hepatocytes in the mouse liver. These human hepatocyte chimeric mice, in which the mouse liver cells were largely (>90%) replaced with human hepatocytes, were used to reduce the potential influence of mouse-derived mRNA on the results obtained. Two mice were each inoculated with purified NC1/SY HCV particles containing 11.6 fmol core protein. The HCV-RNA titer in inoculated mouse serum was monitored by RTD-PCR each week after inoculation.

RESULTS

Genotype 1b HCV clone isolated from a patient with acute severe hepatitis

HCV cDNA was isolated from a patient with acute severe hepatitis. This patient was a 48-year-old woman without any history of blood transfusions. She developed acute severe hepatitis as diagnosed by acute liver failure associated with stage I encephalopathy and low serum prothrombin time (<40%). In the patient's serum, no marker of cytomegalovirus, Epstein-Barr virus, herpes simplex virus, hepatitis A virus or hepatitis B virus was detected. However, only HCV-RNA was detected using RT-PCR analysis, and the virus RNA titer in her serum at admission was 16,660 KIU/mL. The genotype 1b HCV sequence was detected by sequencing analysis of the PCR fragment. The patient was therefore diagnosed as suffering from acute severe hepatitis caused by genotype 1b HCV infection. She received IFN-α treatment, which cleared the viral infection, and she subsequently recovered. The entire sequence of the amplified HCV genomic cDNA was then determined and this HCV strain was designated as NC1. The sequencing analysis indicated that this NC1 strain shared 91.2% nucleotide and 94.4% amino acid sequence homology with the Con1 strain.

Subgenomic replicon analysis of the NC1 strain

To analyze the replication efficiency of the genotype 1b NC1 strain, we constructed the subgenomic replicon, pSGR-NC1, in the form of a Con1 replicon and pSGR-JFH1 (10, 17). This synthesized NC1 replicon RNA was transfected by electroporation into Huh7 or Huh7.5.1 cells. The transfected cells were then grown for 3 weeks in a selection culture that contained 1 mg/mL G418. Several colonies survived this selection culture, as illustrated by crystal violet staining (Fig. 1). The

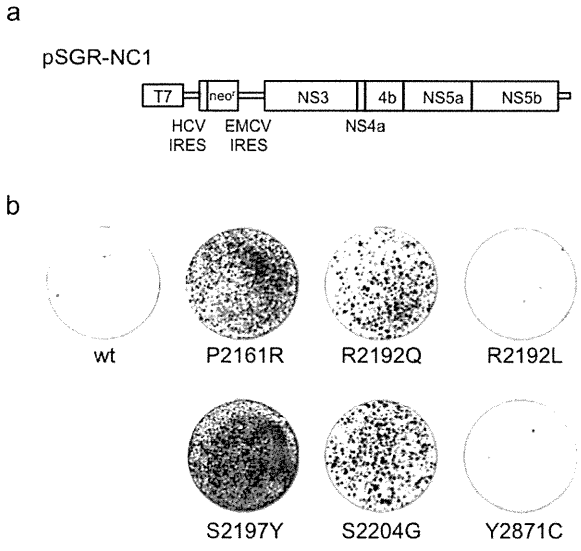

Fig. 1. NC1 subgenomic HCV replicon construct and colony formation of NC1 replicon RNA-transfected Huh7 cells. (a) Organization of the subgenomic replicon construct pSGR-NC1. Open reading frames (wide boxes) are flanked by untranslated regions (narrow boxes). The T7 RNA promoter is located upstream of the 5′ end of the replicon construct. (b) Subgenomic RNAs were synthesized *in vitro* using pSGR-NC1 (wt) and replicon constructs containing one of the mutations P2161R, R2192Q, R2192L, S2197Y, S2204G and Y2871C as templates. Transcribed subgenomic replicon RNAs (3 μg each) were electroporated into Huh7 cells and the cells were cultured with G418 for 3 weeks before staining with crystal violet. Experiments were carried out in triplicate and representative staining examples are shown.

colony-formation efficiency of the NC1 replicons was 1.77 ± 1.54 CFU/μg RNA, which was lower than the colony-formation efficiency of the JFH-1 subgenomic replicon that was determined in our previous study ($5.32 \pm 5.02 \times 10^4$ CFU/μg RNA) (17). Six colonies of the transfected Huh7 cells and 14 colonies of the transfected Huh7.5.1 cells were cloned and expanded for further analysis. Replicon RNA was isolated from each replicon cell clone, and the HCV-RNA titer and sequence of the replicon genome were determined (Table 1). The average HCV-RNA titers in the replicon cell clones derived from Huh7 and Huh7.5.1 cells were determined by RTD-PCR as $4.28 \pm 3.43 \times 10^6$ and $6.72 \pm 7.14 \times 10^6$ copies/μg RNA, respectively.

We next determined the sequence of the replicating replicon genome in each replicon transfected cell clone. All of the clones had at least one non-synonymous mutation and three clones also had a synonymous mutation (Table 1). We found non-synonymous mutations in all of the subgenomic non-structural regions of the replicon genome, and five of the mutations were found in more than one replicon genomic clone. Thus, of the mutations found in the NS5A region, P2161R, R2192L and S2204G mutations were independently detected in two different replicon cell clones, and the S2197Y mutation was detected in three different replicon cell clones. In addition, R2192 was not only mutated to R2192L but was also found as an R2192Q mutation in one replicon. The Y2871C mutation in NS5B was detected in two different replicon cell clones. We therefore selected P2161R, R2192L, R2192Q, S2197Y, S2204G and Y2871C mutations for further analysis to determine their adaptive effects. We inserted P2161R, R2192L, R2192Q, S2197Y, S2204G and Y2871C mutations into the pSGR-NC1 genome and tested

Table 1. Mutations and RNA titer of the NC1 replicon cell clones

Replicon clones†	nt mutation	nt position‡	aa mutation	aa position§	Region	Replicon RNA titer
2	G>A	5302(6916)	R>Q	2192	NS5a	3.58E+05
	T>Y	5490(7104)	S>S,P	2255	NS5a	
5	G>R	4046(5660)	none		NS4b	1.56E+07
	A>G	4088(5702)	I>M	1787	NS4b	
	C>A	5317(6931)	S>Y	2205	NS5a	
	C>S	6579(8193)	Q>Q,E	2618	NS5b	
2–1	T>C	3965(5579)	none		NS4b	3.17E+05
	T>G	5346(6960)	S>A	2207	NS5a	
2–2	C>G	5209(6823)	P>R	2161	NS5a	8.16E+06
2–3	T>C	1721	none		E-I ††	3.97E+06
	C>A	4855(6469)	S>Y	2043	NS5a	
2–5	T>C	3694(5308)	V>C	1656	NS3	1.80E+07
	C>G	5209(6823)	P>R	2161	NS5a	
2–7	G>T	5302(6916)	R>L	2192	NS5a	2.91E+06
2–8	T>C	5067(6681)	C>R	2114	NS5a	1.98E+06
	A>G	7339(8953)	Y>C	2871	NS5b	
2–9	C>A	5317(6931)	S>Y	2197	NS5a	1.58E+07
2–10	A>G	5287(6901)	K>R	2187	NS5a	1.90E+07
	A>G	5337(6951)	S>G	2204	NS5a	
	A>G	7339(8953)	Y>C	2871	NS5b	
2–11	C>A	584	D>E		NEO	2.50E+06
	A>T	3762(5376)	S>C	1679	NS4a	
	T>A	5248(6862)	M>K	2174	NS5a	
2–12	C>T	5291(6905)	none		NS5a	1.02E+06
	G>T	5302(6916)	R>L	2192	NS5a	
2–13	C>A	4850(6464)	N>K	2041	NS5a	3.65E+06
2–15	C>T	5299(6913)	A>V	2191	NS5a	8.07E+05
	A>G	5337(6951)	S>G	2204	NS5a	
	A>G	6014(7628)	none		NS5b	
	A>G	6015(7629)	I>V	2430	NS5b	
H1	C>A	5301(6915)	none		NS5a	1.01E+07
	C>A	5317(6931)	S>Y	2197	NS5a	
H3	G>A	661	G>E		NEO	4.77E+06
	C>A	5323(6937)	A>D	2199	NS5a	
H6	C>A	5265(6879)	H>N	2180	NS5a	1.21E+06
H7	C>A	5308(6922)	S>Y	2194	NS5a	4.53E+05
H10	C>A	5317(6931)	S>Y	2197	NS5a	5.12E+06
H12	A>C	5325(6939)	S>R	2200	NS5a	4.03E+06

†Replicon clones 2~2–15 were derived from Huh7.5.1 cells, and the H1~H12 replicon clones were derived from Huh7 cells. ‡Position within the subgenomic replicon and within full-length NC1 (in parentheses).
§Position within the complete open reading frame of full-length NC1. ¶Copy/μg RNA. ††E-I, EMCV-IRES.

the colony-formation efficiency of the mutant replicons. As shown in Figure 1b, P2161R, R2192Q, S2197Y and S2204G mutations had adaptive effects for colony formation. However, R2192L and Y2871C mutations did not enhance colony-formation efficiency.

Full-length HCV replication

As shown above, some of the mutations detected in the NC1 subgenomic replicon that was transfected into cells exhibited adaptive effects that increased colony-formation efficiency. We next determined whether full-length NC1 HCV clones with these mutations were able to replicate in cultured cells and to produce infectious virus. We therefore introduced the same six mutations that we tested in the subgenomic replicon assay into the full-length NC1 HCV cDNA (Fig. 2a). Full-length viral RNA was synthesized from linearized pNC1 and its mutant derivatives and was electroporated into Huh7.5.1 cells. All of the transfected cells were serially passaged, and HCV core protein levels in the culture supernatant were monitored over time (Fig. 2b). Interestingly, only cells transfected with the NC1 HCV-RNA with an S2197Y or S2204G mutation secreted a significant amount of HCV core protein into the culture medium. Secreted HCV core protein levels reached a maximum at 5–10 days post- transfection and subsequently continuously decreased in the culture medium of the cells transfected with the viral RNA containing S2197Y or S2204G mutation until 32 days after transfection. This reduction in HCV core protein levels after a certain number of cell passages was reproducible and was confirmed in repeated experiments.

Characterization of the NC1 virus particles secreted from NC1 RNA-transfected cells

Of the six NC1 constructs with mutations that were transfected into cells, transfection of NC1/SY RNA, which had the S2197Y mutation, resulted in secretion of the highest level of HCV core protein into the culture medium (Fig. 2b). We therefore further analyzed the HCV particles produced from NC1/SY RNA-transfected cells. Synthesized NC1/SY RNA was transfected again into Huh7.5.1 cells, the transfected cells were passaged and the culture medium was harvested at cell passaging. HCV core protein levels were relatively high in the culture medium from the NC1/SY RNA-transfected cells on days 2 and 15 post-transfection (Table 2). Infectivity of the culture medium was also detected at both time points, although at very low levels (Table 2). We also analyzed HCV core protein in the culture media obtained at these two time points using a density gradient assay. Both media exhibited a high, narrow peak of HCV core protein in fraction 9, which had a density of 1.15 g/mL, as well as a broader

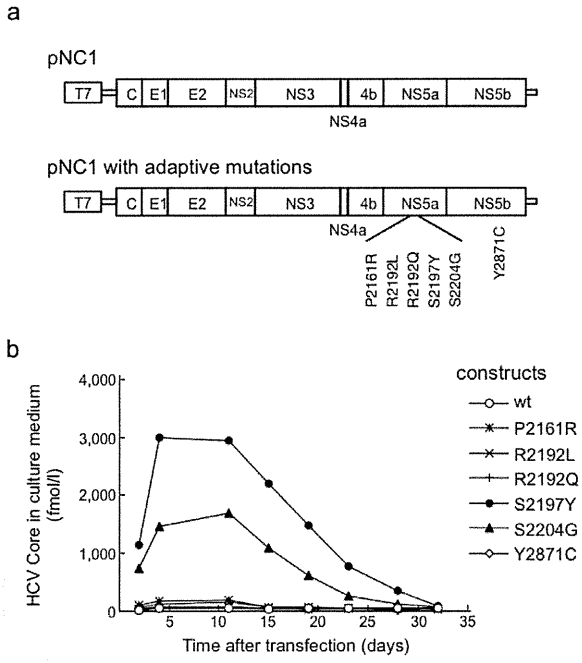

Fig. 2. Analysis of the HCV core protein released into the cell culture medium after transfection of NC1 full-length HCV-RNA. (a) Organization of the full-length NC1construct, pNC1 (upper). Open reading frames (wide boxes) are flanked by untranslated regions (narrow boxes). A T7 RNA promoter is located upstream of the 5′ end of the HCV cDNA construct. Six of the mutations identified in the replicon cell clones were independently introduced into the pNC1 construct (lower). (b) Huh7.5.1 cells were transfected with RNA transcribed from pNC1 with the wild-type HCV sequence (wt) or with RNA from one of the six constructs containing one of the mutations P2161R, R2192Q, R2192L, S2197Y, S2204G or Y2871C. Two independently transfected cell lines were passaged for each construct. At each time point after transfection, the culture medium was harvested and analyzed for the presence of HCV core protein. Average data of duplicate transfections are indicated.

Table 2. HCV core protein and infectivity levels in the culture medium of NC1/SY RNA-transfected cells

Days post-transfection	HCV Core (fmol/L)	Infectivity (ffu/mL)
2	1721	3
15	1009	16

minor peak which had a density of 1.02 to 1.04 g/mL (Fig. 3a). Interestingly, these density gradient profiles were quite similar to the previously described profile of JFH-1 (12). We further identified viral particles in the peak fraction of NC1/SY virus particles obtained following density gradient centrifugation by electron microscopic analysis (Fig. 3b). The observed particles exhibited a spherical shape with diameters of approximately 50–55 nm.

a

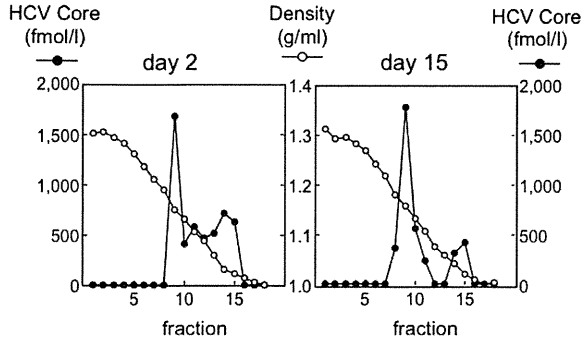

b

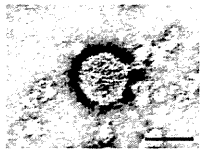

Fig. 3. Characterization of secreted HCV particles from NC1/SY RNA-transfected cells. (a) Sucrose density gradient analysis of the culture supernatant from NC1/SY RNA-transfected Huh7.5.1 cells. One ml of the culture supernatant of transfected cells that was collected on day 2 and day 15 post-transfection (Table 2) was cleared by centrifugation and filtration. Each supernatant was overlaid on a stepwise sucrose density gradient (0, 10, 20, 30, 40, 50 and 60% sucrose) and centrifuged for 16 hrs at 200,000 × *g* at 4°C. Eighteen fractions were collected from the bottom of the tubes and the concentration of HCV core protein in each fraction was determined. Closed and open circles indicate HCV core protein levels (fmol/L) and the sucrose density (g/mL) of the fractions, respectively. (b) Negative-stained HCV particles were observed by electron microscopy. NC1/SY virus particles were purified from the culture medium at 15 days post-transfection and observed by electron microscopy using negative staining. Scale bar, 50 nm.

Infectivity of the NC1/SY virus in human hepatocyte-transplanted uPA/SCID mice

We next determined the *in vivo* infectivity of the NC1/SY virus using human hepatocyte-transplanted uPA/SCID mice, which were reported to be permissive for HCV infection (23). We harvested cell culture media containing NC1/SY virus at 6 days after RNA transfection and was concentrated approximately 20-fold. The concentrated NC1/SY virus was inoculated into two mice designated as PXB 21–39 and PXB 21–40 (Table 3). Human albumin levels in the sera of the inoculated mice were higher than 3 mg/mL during the experiment, which supported the fact that there was a high level of replacement of mouse hepatocytes with human hepatocytes in the mouse liver. Both mice were negative for HCV-RNA at 1 week after inoculation (Table 3). The PXB 21–39 mouse became transiently HCV-RNA positive only at 2 weeks post-inoculation but thereafter remained negative from 3 to 5 weeks post-inoculation. The PXB 21–40 mouse remained HCV-RNA negative until 5 weeks post-inoculation. Thus, the cell culture-adapted NC1/SY virus in the inoculum may have possessed *in vivo* infectivity although this infectivity was at a low level.

Table 3. Serum HCV-RNA titer in human hepatocyte chimeric mice inoculated with the NC1/SY virus produced in cultured cells

Days post-infection	Mouse ID† PXB 21–39	PXB 21–40
7	–	–
14	+	–
21	–	–
28	–	–
35	–	–

†Two mice were independently inoculated with 300 μL NC1/SY (38,600 fmol/L).
+, PCR positive (<2.1×10^4 copies/mL); –, PCR negative.

Combinatory effects of adaptive mutations in different regions

The above experiment showed that NC1/SY RNA-transfected cells could produce infectious virus particles but at very low efficiency. To increase the replication and virus production efficiency of the NC1/SY virus, we tested the effect of introducing additional adaptive mutations into NC1. Thus, the E1202G mutation in NS3 (25) and/or the K1846T mutation in NS4B (26) were introduced into pNC1/SY (Fig. 4a) yielding pNC1/EGSY, pNC1/KTSY and pNC1/EGKTSY. RNAs transcribed from these synthesized constructs were transiently transfected into Huh7.5.1 cells. In this transient transfection experiment, NC1/EGSY and NC1/EGKTSY-RNA-transfected cells expressed higher levels of HCV core protein both in the culture medium and in the cell lysate from 48 to 96 hrs after transfection than cells transfected with RNA of the other NC1 mutants (Fig. 4b and c). However, the NC1/KTSY RNA-transfected cells expressed a similar level of HCV core protein as that expressed by NC1/SY. Interestingly, the E1202G mutation not only increased the level of the HCV core protein but also the infectivity of the culture medium. At 3 days post-transfection, HCV core protein levels reached a concentration of 8193 fmol/L in the medium of NC1/EGSY RNA-transfected cells, and, at the same time point, the infectivity titer in the culture medium of these cells reached 792 ffu/mL (Fig. 4b and Table 4). However, by 25 days post-transfection, the

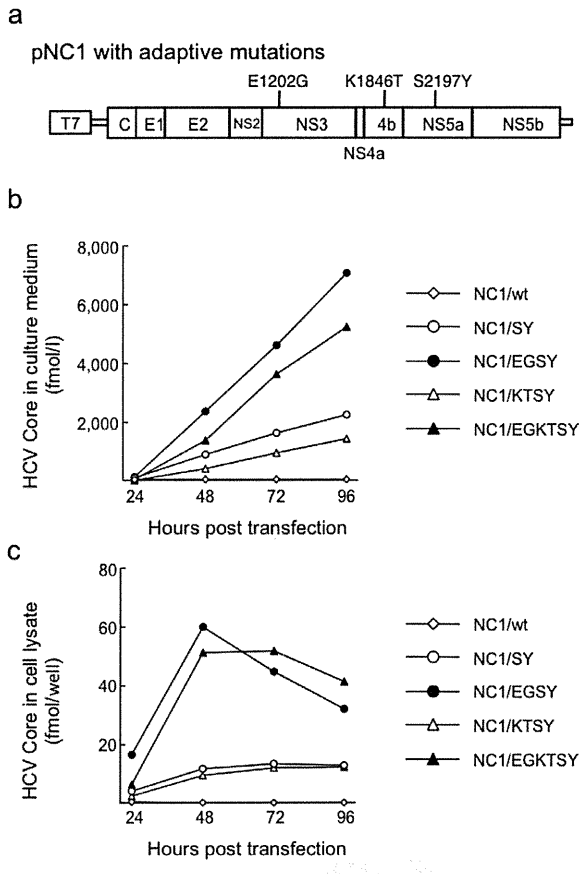

Fig. 4. Kinetics of HCV core protein release into the culture medium and cellular HCV protein expression. (a) Position of the E1202G and K1846T mutations, which were introduced alone or in combination into the full-length pNC1 containing the S2197Y mutation, is shown. Transcribed full-length HCV-RNAs from pNC1 and its mutated derivatives were transfected into Huh7 cells. At each time point, the culture medium and an aliquot of transfected cells were harvested. HCV core protein levels in the culture medium (b) and the cell lysate (c) were determined as described in Materials and Methods. Data indicate the average core protein concentration from two independent transfections. wt, wild type; EG, E1202G; KT, K1846T; SY, S2197Y.

infectivity titer in the culture medium of the NC1/EGSY RNA-transfected cells had decreased to 23.3 ffu/mL. Furthermore, reinfection of the secreted virus did not result in productive infection.

DISCUSSION

In previous studies, we isolated a cell culture infectious genotype 2a HCV strain, the JFH-1 strain, from a patient with fulminant hepatitis (12, 27). In the present study, we isolated a novel genotype 1b HCV cDNA, the NC1 strain. We tested NC1 strain replication efficiency in cultured cells using a drug-selectable subgenomic replicon

Table 4. HCV core protein levels in, and infectivity of, the culture medium of NC1 RNA-transfected cells

Days post-transfection	HCV construct	HCV core (fmol/L)	Infectivity (ffu/mL)
3	NC1/SY	2468	23.3
	NC1/EGSY	8193	792.0
	NC1/KTSY	1079	3.3
	NC1/EGKTSY	5064	467.0
25	NC1/SY	963	3.3
	NC1/EGSY	515	23.3
	NC1/KTSY	319	0.0
	NC1/EGKTSY	995	6.7

assay. Although the colony-forming efficiency of the NC1 replicon was lower than that of JFH-1, we still isolated multiple NC1 replicon cell clones. This result suggested that adaptive mutations in the replicon genome were necessary for efficient replication and that clones that expressed neomycin-resistant gene products were selected. Indeed, some mutations were identified in the NC1 replicon that enhanced colony-formation efficiency (Fig. 1). Notably, the S2197Y and S2204G mutations also increased core protein secretion from cells transfected with full-length NC1 HCV-RNA (Fig. 2). The culture medium of the NC1/SY RNA-transfected cells showed marginal infectivity for naive Huh7.5.1 cells. The *in vivo* infectivity of the NC1/SY virus was confirmed by its inoculation into human hepatocyte-transplanted uPA/SCID mice. Although the *in vivo* NC1/SY virus infectivity was very weak and transient, it was detected in one of the two inoculated mice. By introducing additional adaptive mutations into the NC1/SY virus, we found that a combination of E1202G and S2197Y mutations further enhanced HCV replication and virus production in RNA-transfected cells.

HCV was discovered as a causative agent of non-A, non-B hepatitis in 1989 (1, 2). Since then, efforts to understand the viral life cycle of HCV and to identify effective antiviral agents have been hampered by the lack of an efficient cell culture system for this virus. There have already been many attempts to develop a system for HCV infection and replication in cell culture (reviewed in ref 10). However, the viral replication efficiencies reported in these studies were modest, requiring detection by RT-PCR.

We previously isolated an HCV clone, JFH-1, from a fulminant hepatitis patient with HCV (27). A JFH-1-derived subgenomic replicon proved capable of highly efficient replication in a variety of cell lines (17), and produced infectious HCV particles in Huh7 cells (12–14). The development of an HCV infection system using the JFH-1 strain has contributed to our understanding of this important virus. A genotype 1a strain, H77S, which contained five adaptive mutations, was reported to produce infectious